Quantifying the Hydrophobic Effect. 2. A Computer Simulation−Molecular-Thermodynamic Model for the Micellization of Nonionic Surfactants in Aqueous Solution

Brian C. Stephenson, Arthur Goldsipe, Kenneth J. Beers, and Daniel Blankschtein*

Department of Chemical Engineering, Massachusetts Institute of Technology, Cambridge, Massachusetts 02139

Received: September 1, 2006; In Final Form: November 21, 2006

In this article, the validity and accuracy of the CS−MT model is evaluated by using it to model the micellization behavior of seven nonionic surfactants in aqueous solution. Detailed information about the changes in hydration that occur upon the self-assembly of the surfactants into micelles was obtained through molecular dynamics simulation and subsequently used to compute the hydrophobic driving force for micelle formation. This information has also been used to test, for the first time, approximations made in traditional molecular-thermodynamic modeling. In the CS−MT model, two separate free-energy contributions to the hydrophobic driving force are computed. The first contribution, g_{dehydr}, is the free-energy change associated with the dehydration of each surfactant group upon micelle formation. The second contribution, g_{hydr}, is the change in the hydration free energy of each surfactant group upon micelle formation. To enable the straightforward estimation of g_{dehydr} and g_{hydr} in the case of nonionic surfactants, a number of simplifying approximations were made. Although the CS−MT model can be used to predict a variety of micellar solution properties including the micelle shape, size, and composition, the critical micelle concentration (CMC) was selected for prediction and comparison with experimental CMC data because it depends exponentially on the free energy of micelle formation, and as such, it provides a stringent quantitative test with which to evaluate the predictive accuracy of the CS−MT model. Reasonable agreement between the CMCs predicted by the CS−MT model and the experimental CMCs was obtained for octyl glucoside (OG), dodecyl maltoside (DM), octyl sulfinyl ethanol (OSE), decyl methyl sulfoxide (C_{10}SO), decyl dimethyl phosphine oxide (C_{10}PO), and decanoyl-*n*-methylglucamide (MEGA-10). For five of these surfactants, the CMCs predicted using the CS−MT model were closer to the experimental CMCs than the CMCs predicted using the traditional molecular-thermodynamic (MT) model. In addition, CMCs predicted for mixtures of C_{10}PO and C_{10}SO using the CS−MT model were significantly closer to the experimental CMCs than those predicted using the traditional MT model. For dodecyl octa(ethylene oxide) ($C_{12}E_8$), the CMC predicted by the CS−MT model was not in good agreement with the experimental CMC and with the CMC predicted by the traditional MT model, because the simplifying approximations made to estimate g_{dehydr} and g_{hydr} in this case were not sufficiently accurate. Consequently, we recommend that these simplifying approximations only be used for nonionic surfactants possessing relatively small, non-polymeric heads. For MEGA-10, which is the most structurally complex of the seven nonionic surfactants modeled, the CMC predicted by the CS−MT model (6.55 mM) was found to be in much closer agreement with the experimental CMC (5 mM) than the CMC predicted by the traditional MT model (43.3 mM). Our results suggest that, for complex, small-head nonionic surfactants where it is difficult to accurately quantify the hydrophobic driving force for micelle formation using the traditional MT modeling approach, the CS−MT model is capable of making reasonable predictions of aqueous micellization behavior.

1. Introduction

In article 1 of this series,[1] we developed a computer simulation−molecular-thermodynamic (CS−MT) modeling approach to better understand and quantify the hydrophobic driving force for solute (surfactant and solubilizate) aggregate formation in aqueous solution. As discussed in article 1, a significant body of literature on traditional MT modeling has demonstrated its ability to model the micellization behavior of structurally simple surfactants with quantitative or semiquantitative accuracy.[2−7] In the traditional MT modeling approach, the free-energy change associated with the formation of the surfactant aggregate in aqueous solution is expressed as the sum of several free-energy contributions, all of which can be computed molecularly given the chemical structures of the various micellar components and the solution conditions. To date, traditional MT models of micellization and micellar solubilization have relied on relatively simple approximations for the micellar hydration states of the surfactants and the solubilizates. To extend the applicability of the traditional MT modeling approach to more chemically and structurally complex surfactants and solubilizates, there is a need to accurately estimate the hydration states of these solutes in the micellar state. The CS−MT model represents a novel approach to obtain and analyze this type of hydration data. With the above in mind, in this article, we use the CS−MT model to predict the micellization behavior of nonionic surfactants that are both simple and challenging to model using the traditional MT modeling approach.

1.1. Review of the CS−MT Model. In the CS−MT model, the free energy of aggregate formation, g_{form}, is computed as

* Corresponding author. Department of Chemical Engineering, Room 66-444, Massachusetts Institute of Technology, 77 Massachusetts Avenue, Cambridge, MA 02139. Telephone: (617) 253-4594. Fax: (617) 252-1651. E-mail: dblank@mit.edu

10.1021/jp065697a CCC: $37.00
Published on Web 01/18/2007

the sum of the following six free-energy contributions:[1]

$$g_{\text{form}} = g_{\text{dehydr}} + g_{\text{hydr}} + g_{\text{pack}} + g_{\text{st}} + g_{\text{elec}} + g_{\text{ent}} \quad (1)$$

The physical origin of each of these free-energy contributions can be understood by representing the process of aggregate formation as a thermodynamic cycle consisting of three separate steps (see Figure 2 in article 1). Two of the free-energy contributions in eq 1, g_{dehydr} and g_{hydr}, reflect the hydrophobic free-energy change associated with aggregate formation, or the hydrophobic driving force for micelle formation. In the CS−MT modeling approach, both g_{dehydr} and g_{hydr} are computed using hydration data obtained from computer simulations. The remaining four free-energy contributions (g_{pack}, g_{st}, g_{elec}, and g_{ent}) in eq 1 are computed in the CS−MT model in the same manner as they are computed in the traditional MT modeling approach.[8] However, the way in which g_{pack} and g_{st} are computed could, in principle, be informed by the molecular dynamics simulation data. In article 1, we proposed and validated theoretical models to evaluate g_{dehydr} and g_{hydr}. The free-energy contribution, g_{dehydr}, is computed as follows:[1]

$$g_{\text{dehydr}} = \sum_{i=1}^{n_{\text{hydr}}} (1 - f_i) g_{\text{tr}_i} \quad (2)$$

where n_{hydr} is the total number of hydrophobic groups in the solute, f_i is the fractional hydration of group i, and g_{tr_i} is the free-energy change associated with transferring group i from the aqueous solution to a bulk phase of solute tails. In article 1, we justified computing f for each group i as follows:

$$f = \frac{\text{number of hydrating contacts in the aggregate}}{\text{number of hydrating contacts in bulk water}} \quad (3)$$

where a "hydrating contact" is defined as a contact with an atom that (i) forms hydrogen bonds or (ii) is capable of coordinate (dative covalent) bonding. On the basis of this definition, if a hydrophobic CH_2 group is in contact with the oxygen or hydrogen atoms of a water molecule, a positively charged or a negatively charged ion, or a hydrophilic group in the solute head that is capable of hydrogen bonding, then the contact is considered hydrating. In article 1, we also justified the use of a 0.3 nm cutoff distance to count the hydrating contacts that occur during MD simulation.

The free-energy contribution, g_{hydr}, is computed as follows:[1]

$$g_{\text{hydr}} = \sum_{i=1}^{n_{\text{core}}} \text{SASA}_i f_i \Delta g_{\text{wc}_i} \quad (4)$$

where n_{core} is the total number of hydrophobic groups in the solute that adsorb onto, or penetrate into, the aggregate core, SASA_i is the solvent accessible surface area of group i, and Δg_{wc_i} is defined as the difference in the free energy per unit of solvent accessible surface area associated with the hydration of group i in the micellar state and in the aqueous solution.

In article 1, the CS−MT model was used to calculate the free-energy change associated with the formation of aggregates of octane, dodecane, and hexadecane having various shapes (spheres, cylinders, and slabs) and sizes. In total, five different aggregate geometries were considered for each oil type. To compute g_{form}, f_i data was calculated using information on water contacts obtained by simulating a single oil molecule in bulk water and by simulating the same oil molecule in an oil aggregate. Values of g_{tr_i} were estimated for the CH_2 and the CH_3 groups in each oil molecule from aqueous solubility data of linear alkanes. Values of SASA_i for the CH_2 and the CH_3 groups were estimated using the double cubic lattice method as implemented in GROMACS and a solvent probe of radius 0.2 nm.[9] We also developed an approach to theoretically calculate Δg_{wc_i} for oil molecules, in which Δg_{wc_i} is calculated as the difference between two "microscopic interfacial tensions" or free energies per unit SASA. For oil molecules, Δg_{wc_i} does not depend on i, and is given by[1]

$$\Delta g_{\text{wc}} = \sigma_{\text{core}} - \sigma_{\text{bulk}} = \frac{\sigma A_{\text{core}}}{\text{SASA}_{\text{core}}} - \frac{g_{\text{tr}_i}}{\text{SASA}_i} \quad (5)$$

where σ_{core} is the microscopic "interfacial tension" (interfacial free energy per unit SASA) associated with the aggregate core−water interface, σ_{bulk} is the microscopic "interfacial tension" (interfacial free energy per unit SASA) associated with the group i (CH_2 or CH_3)−water interface in the aqueous solution, σ is the macroscopic interfacial tension of the aggregate core−water interface, A_{core} is the surface area of the hydrophobic aggregate core as computed geometrically based on the volume of the aggregate subject to the assumption of a perfectly smooth aggregate surface, and $\text{SASA}_{\text{core}}$ is the solvent accessible surface area of the hydrophobic aggregate core.

The ratio $A_{\text{core}}/\text{SASA}_{\text{core}}$ in eq 5 was estimated using the following correlation that was fitted on the basis of our computer simulation results for the various oil aggregates considered:[1]

$$\text{SASA}_{\text{core}}/A_{\text{core}} = 1.740 - 0.026 n_{\text{t}} + 0.078 C \quad (6)$$

where n_{t} is the total number of hydrophobic groups in the solute that are part of the hydrophobic aggregate core and C is the curvature of the micellar aggregate, which is defined as $2/l_{\text{c}}$ for spheres, $1/l_{\text{c}}$ for cylinders, and zero for planar interfaces, where l_{c} is the core-minor radius or planar half-width. In article 1, excellent agreement between the predictions of the CS−MT model and the traditional MT model was obtained for g_{form} for each of the 15 oil aggregates modeled, with an average absolute error of only 1.04% between the two modeling approaches. The very high level of agreement between the CS−MT and the traditional MT modeling results demonstrates the ability of the CS−MT model to quantify the hydrophobic effect for completely hydrophobic solutes, as well as to calculate g_{form} with a high degree of accuracy.

In Appendix A of article 1, we showed that, by combining elements of the CS−MT model and the traditional MT model, g_{form} can be computed as a function of aggregate shape and size after performing *only two computer simulations*: the first of the solute in a bulk water environment and the second of the same solute in an aggregate environment (where the aggregate can have arbitrary shape and size). Specifically, we showed that[1]

$$g_{\text{tr,CS-MT}} = g_{\text{dehydr}} + g_{\text{hydr}} - \hat{g}_{\text{int}} \quad (7)$$

where $g_{\text{tr,CS-MT}}$ is the transfer free-energy contribution computed using the CS−MT modeling approach and $\hat{g}_{\text{int}}$ is the traditional MT prediction for the interfacial free-energy contribution of the simulated micellar aggregate. The free energy of aggregate formation, g_{form}, for a micelle of a different shape and size than that at which the computer simulation data was gathered is then calculated using the following equation:[1]

$$g_{\text{form}} = g_{\text{tr,CS-MT}} + g_{\text{int}} + g_{\text{pack}} + g_{\text{st}} + g_{\text{elec}} + g_{\text{ent}} \quad (8)$$

In article 1, we demonstrated that consistent values of $g_{\text{tr,CS-MT}}$ based on hydration information obtained through

computer simulation of oil aggregates of different curvatures can be estimated using eq 7. Using the computed value of $g_{tr,CS-MT}$, we also demonstrated that highly accurate values of g_{form} could be obtained using eq 8 for each of the 15 oil aggregates considered.

For a micelle of the optimum shape, size, composition (in the case of mixed micelles), and degree of counterion binding (in the case of ionic surfactants), g_{form} has a minimum value, which we denote as g^*_{form}. By solving for g^*_{form}, the optimal aggregate shape (S^*), the optimal core-minor radius (l^*_c), the optimal composition (α^*), and the optimal degree of counterion binding (β^*), can be predicted. In addition, the CMC in mole fraction units is computed as follows:[10]

$$\mathrm{CMC} \approx \exp\left(\frac{g^*_{form}(S^*,l^*_c,\alpha^*,\beta^*)}{k_B T}\right) \quad (9)$$

where k_B is the Boltzmann constant and T is the absolute temperature.

1.2. Modeling Nonionic Surfactant Micellization. In this article, we will use the CS−MT modeling approach introduced in article 1 to model the micellization behavior of nonionic surfactants. Although the CS−MT model enables the prediction of a wide range of solution properties, the CMC has been selected for prediction and comparison with the experimental CMC data because the CMC depends exponentially on g_{form}, and as such, it provides a stringent test with which to evaluate the predictive accuracy of the CS−MT model. We have selected the following seven nonionic surfactants in order to test and validate the CS−MT model: octyl glucoside (OG), dodecyl maltoside (DM), octyl sulfinyl ethanol (OSE), decyl methyl sulfoxide ($C_{10}SO$), decyl dimethyl phosphine oxide ($C_{10}PO$), dodecyl octa(ethylene oxide) ($C_{12}E_8$), and decanoyl-*n*-methyl-glucamide (MEGA-10). These seven nonionic surfactants have varying degrees of structural and chemical complexity and, as such, have allowed us to thoroughly gauge the validity and predictive accuracy of the CS−MT modeling approach.

In order to use the CS−MT modeling approach in the case of the nonionic surfactants considered here, we have made three approximations to calculate g_{dehydr} and g_{hydr} in a relatively simple manner. The first approximation involves the way in which we estimate g_{tr_i} to enable the evaluation of g_{dehydr} using eq 2. The second approximation involves introducing an approach to determine which surfactant groups are adsorbed onto, or incorporated within, the micelle core to enable the evaluation of g_{hydr} using eq 4. The third approximation involves using the theoretical model for Δg_{wc}, given in eqs 5 and 6, which was developed for oil molecules, in the case of nonionic surfactants (which are amphiphilic solutes). The validity of these three approximations will be discussed in Section 4.

In addition to determining the validity of the CS−MT model in the case of nonionic surfactants, we will use the detailed hydration information obtained through computer simulation of nonionic surfactant micelles to quantitatively evaluate several of the approximations underlying the traditional MT modeling approach. Specifically, we will evaluate (i) the accuracy of computing the transfer free-energy contribution, g_{tr}, using the head and tail approximations made in the context of the traditional MT modeling approach,[1] and (ii) the extent to which the surfactant heads shield the micelle hydrophobic core from hydrating contacts.

The remainder of this article is organized as follows. Section 2 describes the computer simulation approach that we have used, including an overview of the modeling approach (Section 2.1), the simulation methods and parameters (Section 2.2), and a description of how each system has been prepared and equilibrated (Section 2.3). The data analysis method used to analyze the molecular dynamics trajectories is described in Section 2.4. In Sections 3.1−3.7, computer simulation results are presented for each of the seven nonionic surfactants modeled in this article. In Section 3.8, the accuracy of several approximations made in the traditional MT modeling approach is determined on the basis of the computer simulation results. In Section 4, the CS−MT model and the traditional MT model are used to model the micellization behavior of each of the seven nonionic surfactants considered. Finally, concluding remarks are presented in Section 5.

2. Molecular Dynamics Simulations

2.1. Modeling Approach. To quantify the hydrophobic driving force associated with the formation of nonionic surfactant micelles, we have used atomistic-level computer simulations to determine the change in hydration for each atom (or group of atoms, such as a CH_2 group) upon being transferred from the aqueous solution to the aggregate environment. As described in article 1, this is accomplished by performing two simulations. The first simulation is of a single nonionic surfactant in a simulation cell of water, which we will refer to hereafter as the "bulk water" simulation. The second simulation is of the same nonionic surfactant in a micellar environment, which we will refer to hereafter as the "aggregate" simulation. Each aggregate simulation was prepared by preforming a nonionic surfactant micelle at an arbitrary aggregation number. The nonionic surfactant micelle was simulated for 10 to 15 ns, which provides sufficient time for the surfactant molecules within the micelle to rearrange and come to local equilibrium, but does not provide sufficient time for the surfactant molecules to exit the aggregate environment and enter the aqueous solution. As a result, the computer simulation results do not permit direct prediction of the optimal micelle shape and size that would be observed experimentally. However, as shown in Appendix A of article 1, by using the CS−MT modeling approach, obtaining information about the hydration state of a micelle of a single shape and size is sufficient to allow prediction of the *optimal* micelle shape and size.

2.2. Simulation Methods and Parameters. The simulation methods and parameters used here are identical to those described in article 1, where we provided a detailed description of the simulation methodology.[1,14−19] Each of the nonionic surfactants was modeled using the fully atomistic OPLS-AA force field,[11] and water was modeled using the simple extended point-charge (SPC/E) model. For the nonionic surfactants OG, DM, and $C_{12}E_8$, atomic charges were assigned on the basis of the default atomic charge values recommended in OPLS-AA. However, because the OSE, $C_{10}SO$, $C_{10}PO$, and MEGA-10 surfactant head structures did not have suggested charges in the OPLS-AA force field, we estimated the atomic charges for these heads using the CHelpG algorithm (as implemented in Gaussian 98), in which atomic charges are assigned to fit electrostatic potentials at a number of points on the van der Waals surface.[12] We note that CHelpG was *not* used to assign atomic charges for the hydrophobic tails of these four surfactants. In a separate study, we determined that assigning atomic charges to the CH_2 and the CH_3 groups in a linear alkyl chain using CHelpG yields simulation results that are less physically realistic than those obtained by assigning atomic charges with the recommended OPLS-AA charges (results not shown).

In two recent publications, we investigated the sensitivity of the head and tail assignments obtained through computer

TABLE 1: Overview of the MD Simulations[a]

surfactant	number of surfactant molecules	number of water molecules	total number of atoms
OG	29	3695	12477
DM	45	4283	16494
OSE	25	3750	12125
$C_{12}E_8$	41	15256	49663
$C_{10}PO$	50	6708	22174
$C_{10}SO$	50	3510	12380
MEGA−10	42	3351	12531

[a] The number of surfactant and water molecules and the total number of atoms corresponding to each of the seven simulated nonionic surfactant micelles are listed.

simulation to the method used to assign atomic charges.[13,14] In general, we found that the results are sensitive to the atomic charges used and that the charge assignments recommended within the OPLS-AA force field yield more reasonable results than those obtained using the CHelpG algorithm. However, if a specific surfactant or solubilizate does not have suggested charges in the OPLS-AA force field, we found that applying the CHelpG approach to determine charges yields reasonably accurate results.

2.3. System Preparation and Equilibration. *2.3.1. Bulk Water Simulation.* The bulk water simulation for each of the nonionic surfactants considered was initialized by placing a single surfactant molecule in a simulation cell and surrounding it with water molecules. The simulation cell was selected to be sufficiently large that there was always at least 2.0 nm of water separating the surfactant molecule from its periodic image, where this simulation cell size was justified in article 1.[1] After brief equilibration under *NPT* conditions until the system volume had stabilized, a 2 to 5 ns data-gathering simulation was carried out.

2.3.2. Aggregate Simulation. The method used to carry out each of the surfactant aggregate simulations was more complex. Each nonionic surfactant micelle was preformed as a spherical aggregate by placing a number of surfactant molecules in close proximity with each surfactant head oriented radially outward from the micelle center. The surfactant molecules were placed such that the surfactant heads were approximately uniformly spaced at the micelle surface. Next, sufficient water molecules were added around each micelle such that it was separated by at least 2 nm from its periodic image. A relatively large simulation cell size was required for $C_{12}E_8$ because of the large size of its polymeric E_8 head. The number of surfactant and water molecules and the total number of atoms included in the simulation cell for each nonionic surfactant micelle are listed in Table 1.

Selection of the Simulation Geometry. At this point, it is worth discussing why spherical, rather than cylindrical or bilayer, micelles were selected for simulation. As shown in Appendix A of article 1, any aggregation number and aggregate geometry (whether spherical, cylindrical, or planar) may be used to obtain hydration information for input to the CS−MT modeling approach.[1] An infinite cylinder or bilayer can be modeled in a computationally efficient manner by simulating only a small cross section of the cylinder or bilayer. We have selected spherical geometries for simulation, however, because carrying out physically realistic cylindrical and bilayer simulations requires that each surfactant molecule has a physically realistic area available to it at the micelle core−water interface (which we will refer to hereafter as *a*) for the simulated micelles to remain stable. The equilibrium area per surfactant head in a micelle results from a complex interplay of forces (including steric, electrostatic, van der Waals, and hydrogen-bonding interactions). If *a* for a preformed spherical micelle is too small, then the micelle will simply become somewhat ellipsoidal during simulation. On the other hand, if *a* for a preformed cylindrical or bilayer micelle is too small, the simulation cell dimensions must be allowed to expand or the micelle will buckle during the simulation and may break apart. If *a* is much larger than the experimental value, a spherical micelle will remain stable on the simulation timescales involved in CS−MT modeling, but a cylindrical micelle or bilayer may break up to form smaller spherical or ellipsoidal aggregates during simulation. In addition to these stability concerns, we note that if *a* is very different from the experimental value, we expect that eqs 7 and 8, in which $g_{tr,CS-MT}$ is assumed to be constant and not to be a function of micelle shape and size, may not be valid.

An appropriate value of *a* for each surfactant molecule in a cylindrical or planar aggregate can be determined through computer simulation by performing constant volume simulations of a number of cylindrical or planar aggregates preformed with different *a* values and using the computer simulation results to identify the value of *a* that yields the minimum energy of interface formation. Such an approach was implemented recently by Jang et al. in determining an appropriate *a* value for simulation of Newton black films.[20] An alternative approach to ensure that cylindrical or bilayer micelles are simulated with a reasonable value of *a* for each surfactant head is to preform the micelle at an arbitrary value of *a* per surfactant molecule but then allow the simulation cell dimensions to change during simulation subject to physically realistic boundary conditions. Unfortunately, such boundary conditions are difficult to determine. The appropriate boundary condition to use parallel to the axis of a cylindrical micelle, or parallel to the surface of a bilayer micelle, is a surface tension that provides a post-equilibration value of *a* that is similar to the one that would be observed experimentally. Particularly in the case of bilayer simulations, one might assume that macroscopic surface tension data could be used to infer the appropriate surface tension value for use during simulation. However, it is known that macroscopically observed surface tensions are difficult to predict accurately from a microscopic simulation.[21,22] A major reason for this is that long (micron) wavelength undulations are not included in nanometer-scale simulation results. Other researchers have commented on this limitation and used it to justify applying nonzero surface tensions in flaccid lipid bilayer simulations where the appropriate macroscopic surface tension is arguably zero.[22] Accordingly, a macroscopic surface tension is not likely to be appropriate for use as a boundary condition during cylindrical or bilayer micelle simulation.

Clearly, the simulation of cylindrical or bilayer aggregates introduces complications that are not present during simulation of spherical aggregates. With these complications in mind, we chose to preform each surfactant micelle in a spherical geometry in aqueous solution. Each of the nonionic surfactant micelles was constructed with an aggregation number sufficiently small to ensure that it would exist as a spherical aggregate during simulation. For several surfactants (OG, DM, $C_{12}E_8$, and MEGA-10), this was accomplished by estimating the expected aggregation number of a spherical micelle given the head area and tail volume of each surfactant molecule.[23] For other surfactants (OSE, $C_{10}PO$, and $C_{10}SO$), the surfactant head area is sufficiently small that we would expect them to form cylindrical micelles with a potentially large aggregation number.[23] Therefore, for each of these three surfactants, spherical

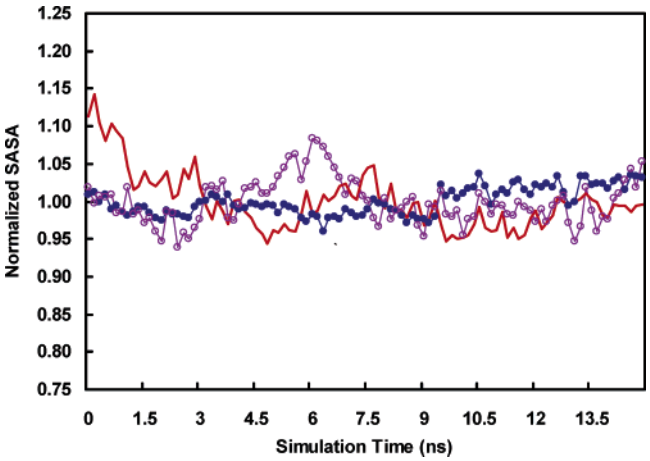

Figure 1. Solvent accessible surface area (SASA) normalized by the average value of SASA as a function of simulation time for micelles of three representative nonionic surfactants: dodecyl maltoside (DM, −●−), dodecyl octa(ethylene oxide) ($C_{12}E_8$, −○−), and decanoyl-*n*-methylglucamide (MEGA-10, −).

micelles were preformed with an aggregation number that was selected arbitrarily.

Micelle Equilibration. After preforming each spherical micelle, an energy minimization was conducted to remove close contacts. Next, an extended equilibration run under *NPT* conditions was conducted for 10 ns. Results by other researchers when conducting atomistic-level simulations of micelles in aqueous solution suggest that a simulation time of 10 ns should be more than adequate to equilibrate a spherical micelle.[24] One measure of equilibration for micellar systems is whether or not each group in a surfactant molecule has come to an equilibrium distance from the micelle center-of-mass. Bruce et al. have reported that sodium counterions are the slowest component of an SDS surfactant−water system to come to an equilibrium distance from the SDS micelle center-of-mass, taking only about 1 ns to equilibrate.[24] For the nonionic surfactants considered here, no counterions were present. Equilibration was confirmed from our simulation results by monitoring the total potential energy (which became stable during a small fraction of the total simulation time) and the solvent accessible surface area (SASA) of the micelle, where SASA was computed using the double cubic lattice method as implemented in GROMACS. The solvent accessible surface was traced out by a probe sphere of radius 0.2 nm (as justified in article 1)[1] that was rolled around each molecule within the aggregate to identify the solvent accessible region.[9] We consider SASA to be the most important metric to measure equilibration because this property is directly proportional to the degree of hydration of the micelle, and obtaining accurate hydration information is the central objective of our computer simulations. Plots of the SASA profiles for three representative nonionic surfactants (DM, $C_{12}E_8$, and MEGA-10) during equilibration are shown in Figure 1. The SASA values reported in Figure 1 for each surfactant have been normalized by the average SASA value for that surfactant to facilitate comparison of the results. The lack of noticeable drift in SASA toward the end of the 10 ns equilibration simulation run confirms that water contact data gathered during the subsequent 5 ns of data gathering should be representative of the hydration state of the micelle in its equilibrium configuration. Plots of the normalized SASA values over the course of the 5 ns data-gathering simulation runs for each surfactant are presented in the Supporting Information.

Snapshots of the post-equilibration configurations of each simulated nonionic micelle are shown in Figure 2. Each surfactant molecule is depicted using the van der Waals radius of each atom. For clarity, the water molecules are not shown.

2.4. Data Analysis Method. To quantify the degree of hydration of each atom (or group of atoms) in the surfactant molecule during the bulk water simulation, the number of contacts with hydrogen-bonding or with coordinate (dative covalent) bonding atoms per time step experienced by each atom was counted over the course of a simulation run, as justified in article 1.[1] For the nonionic surfactants considered in this article, contacts with both water atoms and with hydrogen-bonding surfactant headgroups have been counted as contributing to hydration. In analyzing our simulation data, a contact was defined as two atoms separated by less than 0.3 nm (the "cutoff" distance) at any time during the simulation. The average number of contacts is directly proportional to the average number of hydrogen or coordinate bonding atoms located within the cutoff distance. The degree of hydration of the surfactant molecules during the aggregate simulations was quantified in the same manner and with the same 0.3 nm cutoff distance used in analyzing the results of the bulk water simulation. From the contacts data obtained in this manner, we computed *f*, the fractional degree of hydration of each surfactant atom (or group of atoms), which is the key computer simulation input to the CS−MT model (see eq 3).

Although a cutoff of 0.3 nm was used to determine the hydration data for CS−MT modeling (which includes only *f* values for CH, CH_2, and CH_3 groups), a cutoff of 0.5 nm was used to generate the hydration plots presented in Section 3. Using a larger cutoff when generating the hydration plots improved the statistics of the *f* values obtained for several of the large atoms present in the surfactant heads (including nitrogen, sulfur, phosphorus, and oxygen).

An estimate of the standard error in *f* for each group of atoms in the surfactant molecule was made through block averaging, a useful approach to analyze correlated data.[25−27] A detailed discussion of this error analysis approach was presented in article 1.[1] Data-gathering simulation runs for each surfactant molecule in the bulk water and in the aggregate states were conducted for sufficient time to ensure that the uncertainty in each calculated value of *f* was small—typically less than 5%.

3. Simulation Results and Discussion

In this section, computer simulation results for fractional hydration are presented for each of the seven nonionic surfactants considered in this article. In addition to the *f* values computed using eq 3, two other fractional hydration values were computed: (i) *f* values in which the only contacts in the aggregate state that were counted as hydrating were water contacts (denoted as f_{water}) and (ii) *f* values in which the only contacts in the aggregate state that were counted as hydrating were contacts with hydrogen-bonding groups in the surfactant heads (denoted as f_{head}), where

$$f = f_{water} + f_{head} \tag{10}$$

We have computed values of f_{water} and f_{head} to gain insight into (i) the extent to which contacts with hydrophilic groups in the head contribute to the hydration of hydrophobic atoms in each surfactant head and tail and (ii) to determine whether *f* or f_{water} values are most appropriate to use in the CS−MT modeling approach. We can evaluate (i) on the basis of the hydration results for each surfactant presented in this section (see Figures 3−9). We will discuss (ii) in greater detail in Section 4.10, where

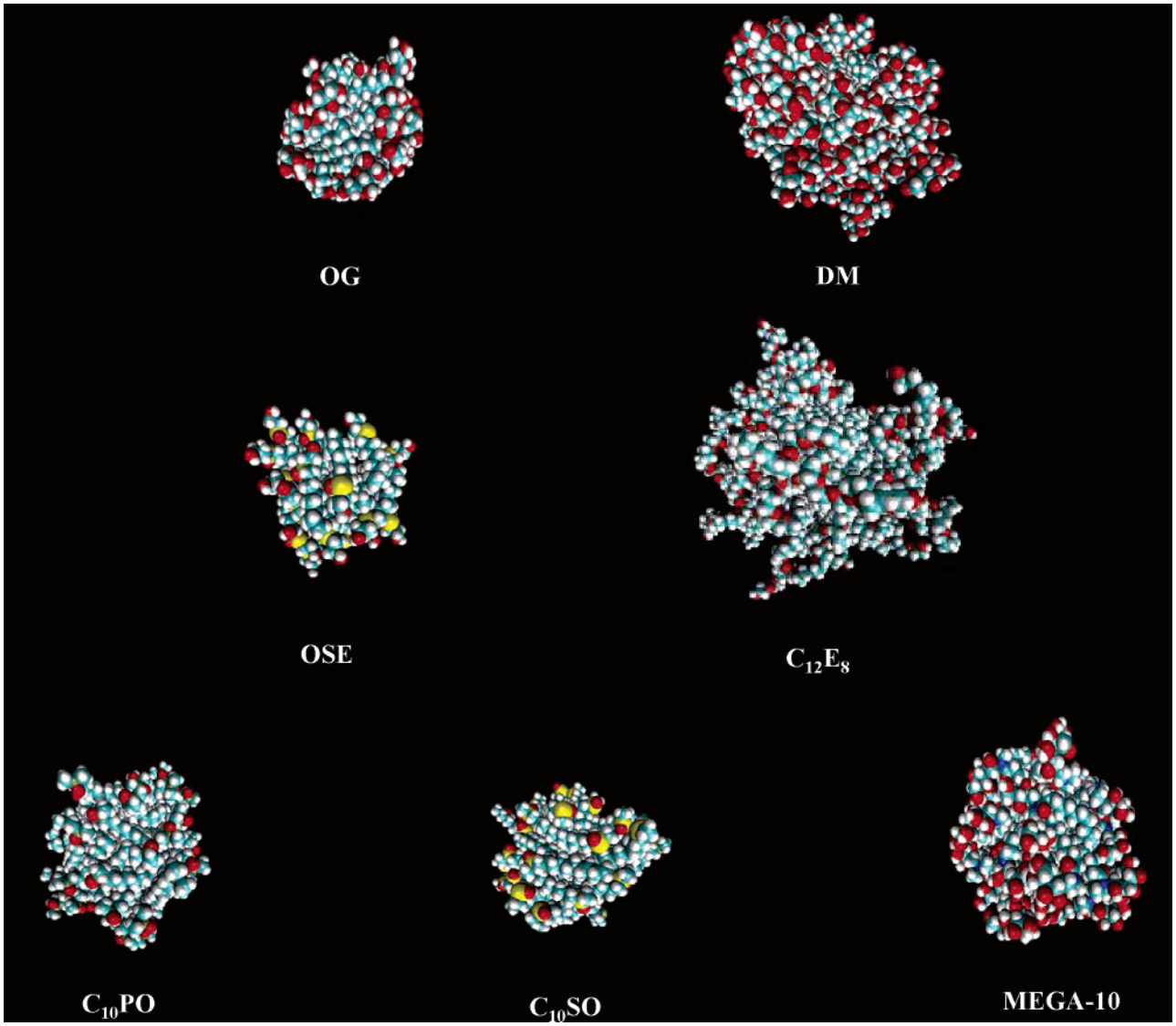

Figure 2. Snapshots of the post-equilibration structures of the seven simulated micelles considered here. The water molecules are not shown for clarity.

CS−MT modeling results obtained using f and f_{water} values will be compared.

3.1. Octyl Glucoside (OG). The fractional degree of hydration of OG is plotted as a function of group number in Figure 3. Three different fractional hydration profiles (f, f_{water}, and f_{head}) are shown in the figure. Hydrophilic and hydrophobic groups that are considered to be part of the OG head in traditional MT modeling (groups 1−12) have f values (see the −♦− results) that are much larger than the f values of groups in the OG tail (groups 13−20). However, to some extent, each group in the OG head is partially dehydrated and has an f value that is less than 1.0. The average f value of the groups in the OG head is 0.69. Clearly, the approximation made in traditional MT modeling that the surfactant head remains completely hydrated is not very accurate, although we note that for simple surfactants, the traditional MT modeling approach yields quantitatively, or semiquantitatively, accurate predictions of the micellization behavior.[2,3,8,10]

The f results in Figure 3 show that the degree of dehydration of the groups in the surfactant head is a function of their distance from the surfactant tail. For example, oxygen atom 12 (closest to the tail) has an f value of 0.4, and oxygen atom 10 has an f value of 0.7. Similarly, the degree of dehydration of the groups in the surfactant tail is a function of their distance from the surfactant head. For example, the CH_2 group closest to the head (group 13) has an f value of 0.41, and the next CH_2 group (group 14) has an f value of 0.25. The average f value of the groups in the OG tail is 0.24.

Although most of the hydrating contacts experienced by the atoms in the OG tail are made with water, these atoms also make a significant number of contacts with hydrogen-bonding atoms in the OG head (groups 1, 3, 5, 7, 10, and 12). The average value of f_{water} (−■−) of the groups in the OG tail is 0.18, and the average value of f_{head} (−▲−) of the groups in the OG tail is 0.07. Clearly, the value of $g_{tr,CS-MT}$ that is computed in the CS−MT model will depend strongly on whether or not hydrogen-bonding atoms in the surfactant head are modeled as contributing to hydration or, in other words, on whether f or f_{water} is used in eqs 2 and 4.

3.2. Dodecyl Maltoside (DM). The fractional degree of hydration of DM is plotted as a function of group number in Figure 4. Three different fractional hydration profiles (f, f_{water}, and f_{head}) are shown in the figure. The same general trends in f (see the −♦− results), f_{water} (−■−), and f_{head} (−▲−) that are observed for OG are observed for DM. It is interesting to note, however, that the average f value of the groups in the DM tail

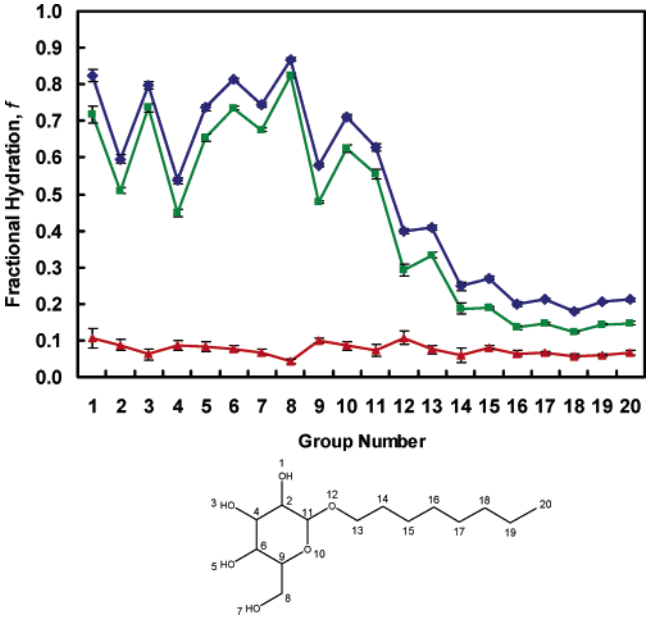

Figure 3. The average fractional degree of hydration, *f*, as defined in eq 3, for each of the groups in octyl glucoside (OG). Results are reported for fractional hydration values computed on the basis of counting contacts with water and with hydrogen-bonding groups in the surfactant head in the aggregate state (*f*, −◆−), for fractional hydration values on the basis of counting contacts only with water in the aggregate state (f_{water}, −■−), and for fractional hydration values on the basis of counting contacts only with hydrogen-bonding groups in the surfactant head in the aggregate state (f_{head}, −▲−). The chemical structure associated with each group is identified in the schematic of the molecule shown below the fractional hydration plot. The error bars shown correspond to the standard error of the mean.

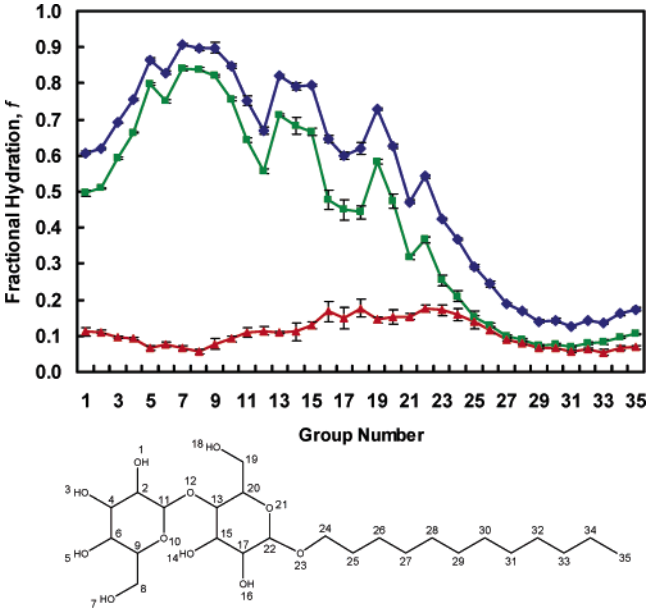

Figure 4. The average fractional degree of hydration, *f*, as defined in eq 3, for each of the groups in dodecyl maltoside (DM). Results are reported for fractional hydration values computed on the basis of counting contacts with water and with hydrogen-bonding groups in the surfactant head in the aggregate state (*f*, −◆−), for fractional hydration values on the basis of counting contacts only with water in the aggregate state (f_{water}, −■−), and for fractional hydration values on the basis of counting contacts only with hydrogen-bonding groups in the surfactant head in the aggregate state (f_{head}, −▲−). The chemical structure associated with each group is identified in the schematic of the molecule shown below the fractional hydration plot. The error bars shown correspond to the standard error of the mean.

(groups 24−35) is 0.19, which is significantly lower than the average *f* value of the groups in the OG tail (0.24). The DM tail is most likely less hydrated than the OG tail, on average, because the simulated DM micelle has a larger l_c value than the OG micelle, imparting to the hydrophobic core a lower surface area to volume ratio. The average *f* value of the groups in the DM head (groups 1−20) is 0.71, which is very similar to that of the OG head (0.69).

An interesting difference between the f_{head} profiles for OG and DM is that the average value of f_{head} for groups in the second ring structure in the DM head (groups 13−22), at 0.16, is significantly larger than the average value of f_{head} in the first ring of the DM head (groups 1−11), at 0.09. It is also significantly larger than the average value of f_{head} for the ring structure of the OG head (groups 1−11), at 0.08. The larger values of f_{head} experienced by groups 13−22 is most likely due to these groups being exposed to a higher concentration of hydrogen-bonding head groups than groups 1−11 in OG or in DM. Inspection of the contacts data shows that, although head contacts account for only 28% of the total hydrating contacts in OG, they account for 35% of the total hydrating contacts in DM. From these observations, the use of f_{water} values, rather than *f* values, in eqs 2 and 4 for CS−MT modeling is expected to have an even greater effect on the modeling results for DM than for OG.

3.3. Octyl Sulfinyl Ethanol (OSE). Fractional degree of hydration results (*f*, f_{water}, and f_{head}) for OSE are plotted as a function of group number in Figure 5. The average value of *f* (see the −♦− results) for the OSE head (0.73) is similar to that for the OG and the DM heads (0.69 and 0.71, respectively). However, the average value of f_{head} (−▲−) for OSE (0.04) is smaller than that for OG (0.08) and DM (0.11). This could be

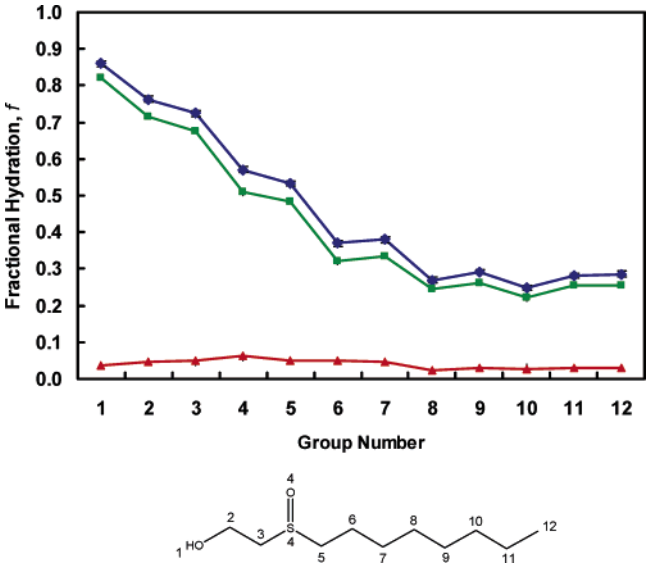

Figure 5. The average fractional degree of hydration, *f*, as defined in eq 3, for each of the groups in octyl sulfinyl ethanol (OSE). Results are reported for fractional hydration values computed on the basis of counting contacts with water and with hydrogen-bonding groups in the surfactant head in the aggregate state (*f*, −♦−), for fractional hydration values on the basis of counting contacts only with water in the aggregate state (f_{water}, −■−), and for fractional hydration values on the basis of counting contacts only with hydrogen-bonding groups in the surfactant head in the aggregate state (f_{head}, −▲−). The chemical structure associated with each group is identified in the schematic of the molecule shown below the fractional hydration plot. The error bars shown correspond to the standard error of the mean.

due to a lower concentration of hydrogen-bonding groups at the OSE micelle surface and to a lower affinity of the hydrogen-

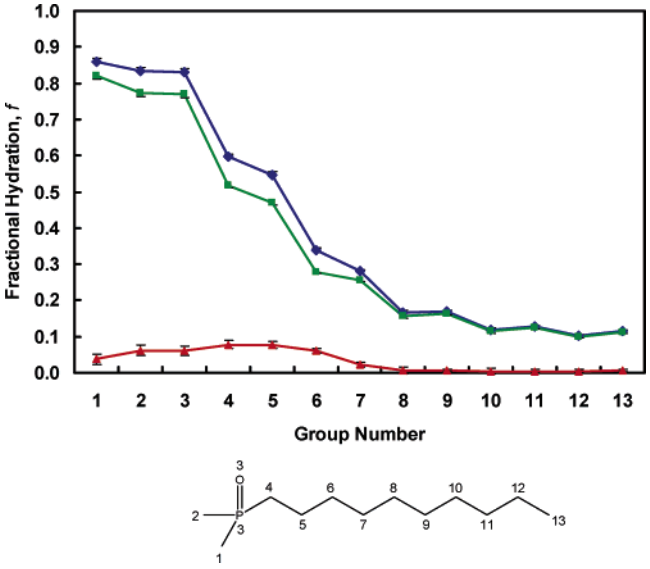

Figure 6. The average fractional degree of hydration, *f*, as defined in eq 3, for each of the groups in decyl dimethyl phosphine oxide (C_{10}PO). Results are reported for fractional hydration values computed on the basis of counting contacts with water and with hydrogen-bonding groups in the surfactant head in the aggregate state (*f*, −◆−), for fractional hydration values on the basis of counting contacts only with water in the aggregate state (f_{water}, −■−), and for fractional hydration values on the basis of counting contacts only with hydrogen-bonding groups in the surfactant head in the aggregate state (f_{head}, −▲−). The chemical structure associated with each group is identified in the schematic of the molecule shown below the fractional hydration plot. The error bars shown correspond to the standard error of the mean.

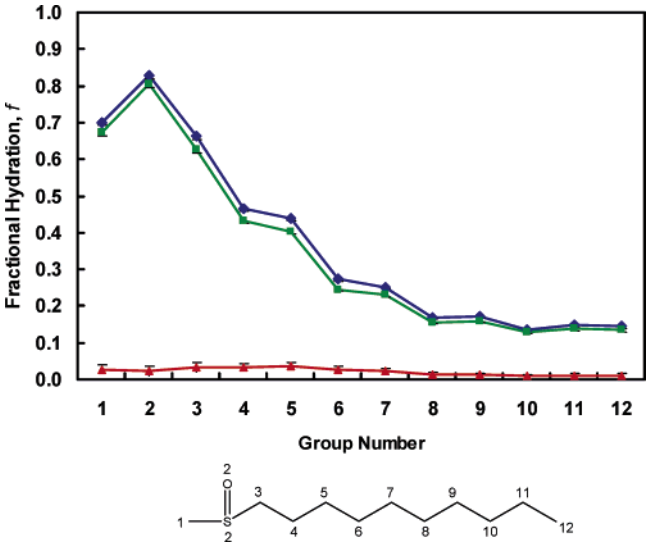

Figure 7. The average fractional degree of hydration, *f*, as defined in eq 3, for each of the groups in decyl ethyl sulfoxide (C_{10}SO). Results are reported for fractional hydration values computed on the basis of counting contacts with water and with hydrogen-bonding groups in the surfactant head in the aggregate state (*f*, −◆−), for fractional hydration values on the basis of counting contacts only with water in the aggregate state (f_{water}, −■−), and for fractional hydration values on the basis of counting contacts only with hydrogen-bonding groups in the surfactant head in the aggregate state (f_{head}, −▲−). The chemical structure associated with each group is identified in the schematic of the molecule shown below the fractional hydration plot. The error bars shown correspond to the standard error of the mean.

bonding groups for each other. The average value of *f* for the OSE tail groups (0.33) is more similar to that of OG (0.24) than to that of DM (0.19). It is interesting to note that the average value of *f* for the OSE tail groups is higher than that for the

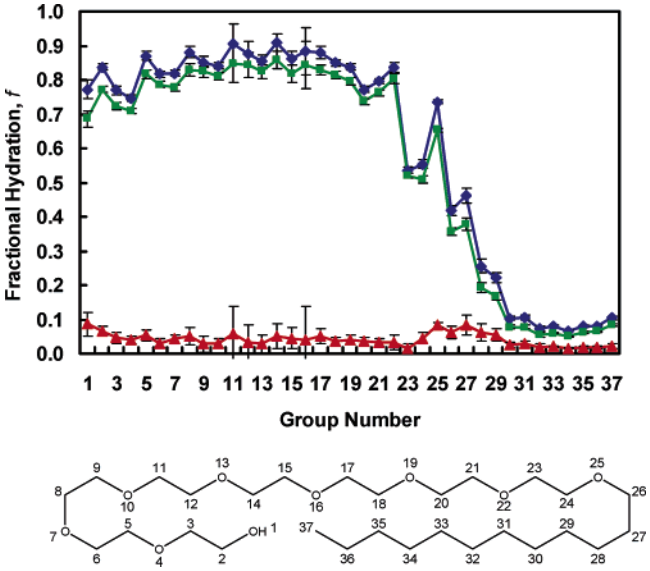

Figure 8. The average fractional degree of hydration, *f*, as defined in eq 3, for each of the groups in dodecyl octa(ethylene oxide) ($C_{12}E_8$). Results are reported for fractional hydration values computed on the basis of counting contacts with water and with hydrogen-bonding groups in the surfactant head in the aggregate state (*f*, −◆−), for fractional hydration values on the basis of counting contacts only with water in the aggregate state (f_{water}, −■−), and for fractional hydration values on the basis of counting contacts only with hydrogen-bonding groups in the surfactant head in the aggregate state (f_{head}, −▲−). The chemical structure associated with each group is identified in the schematic of the molecule shown below the fractional hydration plot. The error bars shown correspond to the standard error of the mean.

OG tail groups, indicating that the OSE micelle core is more hydrated than the OG micelle core, despite the fact that the simulated OSE micelle has a slightly smaller micelle core (l_c = 1.13 nm) than the simulated OG micelle (l_c = 1.19 nm). This comparatively high degree of hydration is due to the relatively large *f* values observed for hydrophobic groups 5, 6, and 7 in OSE relative to groups 13, 14, and 15 in OG.

It is interesting to note that the *f* values of groups 2 and 3, which are hydrophobic, are larger than that of group 4, which is hydrophilic. Clearly, the position of a group within a surfactant molecule (and therefore, relative to the micelle core), in addition to its chemical identity, is of importance in determining the degree of dehydration that it experiences upon micelle formation.

3.4. Decyl Dimethyl Phosphine Oxide (C_{10}PO). Fractional degree of hydration results (*f*, f_{water}, and f_{head}) for C_{10}PO are plotted as a function of group number in Figure 6. The average *f* values of the C_{10}PO head groups (groups 1−3) and the C_{10}PO tail groups (groups 4−13) are 0.84 and 0.26, respectively (see the −◆− results). The degree of hydration of the C_{10}PO head is higher than that observed in OG, DM, and OSE. It is interesting to note that groups 1, 2, and 3 have similar *f* values despite the hydrophobic character of groups 1 and 2. In addition, the average *f* value of the C_{10}PO tail groups (0.26) is significantly larger than that of the DM tail groups (0.19), despite the fact that the simulated C_{10}PO micelle is somewhat smaller (l_c = 1.52) than the simulated DM micelle (l_c = 1.56). This comparatively high degree of hydration is due to the relatively large *f* values observed for hydrophobic groups 4, 5, and 6 in C_{10}PO relative to groups 24, 25, and 26 in DM.

3.5. Decyl Methyl Sulfoxide (C_{10}SO). Fractional degree of hydration results (*f*, f_{water}, and f_{head}) for C_{10}SO are plotted as a function of group number in Figure 7. The average *f* values (see the −◆− results) of the C_{10}SO head groups (groups 1 and 2) and the C_{10}SO tail groups (groups 3−12) are 0.76 and 0.29,

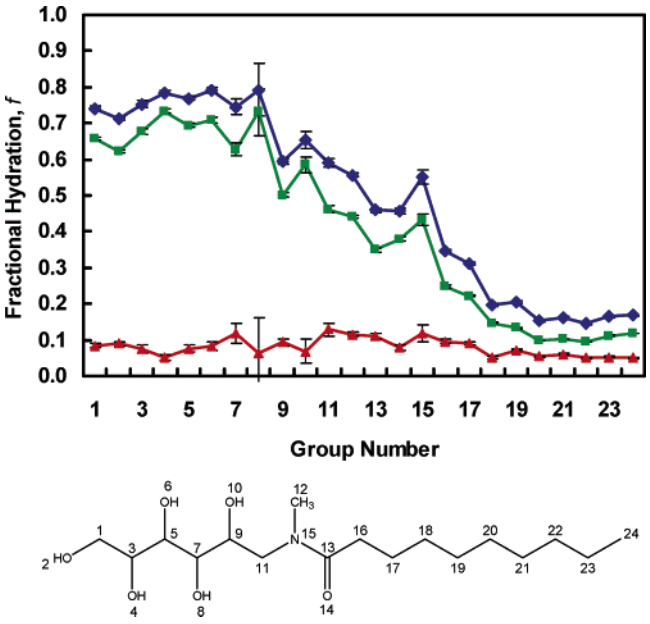

Figure 9. The average fractional degree of hydration, *f*, as defined in eq 3, for each of the groups in decanoyl-*n*-methylglucamide (MEGA-10). Results are reported for fractional hydration values computed on the basis of counting contacts with water and with hydrogen-bonding groups in the surfactant head in the aggregate state (*f*, −◆−), for fractional hydration values on the basis of counting contacts only with water in the aggregate state (f_{water}, −■−), and for fractional hydration values on the basis of counting contacts only with hydrogen-bonding groups in the surfactant head in the aggregate state (f_{head}, −▲−). The chemical structure associated with each group is identified in the schematic of the molecule shown below the fractional hydration plot. The error bars shown correspond to the standard error of the mean.

respectively. In contrast to the results obtained for CH_3 groups 1 and 2 in $C_{10}PO$, the hydrophobic CH_3 group 1 in $C_{10}SO$ has a lower *f* value than the hydrophilic groups in the head (groups 3 and 2 for $C_{10}PO$ and $C_{10}SO$, respectively). This difference between $C_{10}PO$ and $C_{10}SO$ may reflect differences in the atomic charges of the two surfactant heads. Despite the superficial chemical similarity of these two head groups, the atomic charges predicted using the CHelpG algorithm for the two heads are quite different, with $C_{10}PO$ having a charge distribution that makes its dipole moment roughly twice as large as that of $C_{10}SO$. Differences in the hydration profiles of the $C_{10}PO$ and the $C_{10}SO$ tails could be due both to differences in the head atomic charges and to differences in the shape and size of the two surfactant heads.

3.6. Dodecyl Octa(Ethylene Oxide) ($C_{12}E_8$). Fractional degree of hydration results (*f*, f_{water}, and f_{head}) for $C_{12}E_8$ are plotted as a function of group number in Figure 8. The average *f* values (see the −◆− results) of the $C_{12}E_8$ head groups (groups 1−25) and the $C_{12}E_8$ tail groups (groups 26−37) are 0.81 and 0.17, respectively. The small average degree of hydration of the hydrophobic core can be explained by the relatively large size of the micelle hydrophobic core (l_c = 1.51 nm), which is similar to that of the simulated DM micelle (l_c = 1.56 nm).

Because $C_{12}E_8$ and DM both have relatively large heads and the same hydrocarbon tail length, it is instructive to compare the fractional hydration results for $C_{12}E_8$ and DM. The most striking difference between the fractional hydration profiles of $C_{12}E_8$ and DM is the relatively low f_{head} values (−▲−) observed for the $C_{12}E_8$ head groups. The average value of f_{head} for the $C_{12}E_8$ head groups (groups 1−25), which have an average value of 0.04, is significantly smaller than the average value of f_{head} for the DM head groups (0.12). A possible explanation for this difference is that the hydrogen-bonding groups in the $C_{12}E_8$ head are not as attracted to each other as are the head groups in DM. The DM head contains both hydrogen bond donors and acceptors, and the $C_{12}E_8$ head contains several hydrogen bond acceptors but only a single hydrogen bond donor (OH group 1). Therefore, a DM head is capable of forming hydrogen bonds with both water and with other DM heads; a $C_{12}E_8$ head primarily forms hydrogen bonds with water, a difference that is expected to lower the average value of f_{head} of $C_{12}E_8$ relative to that of DM.

3.7. Decanoyl-*n*-Methylglucamide (MEGA-10). Fractional degree of hydration results (*f*, f_{water}, and f_{head}) for MEGA-10 are plotted as a function of group number in Figure 9. The average *f* value (see the −◆− results) of the groups in the MEGA-10 tail (groups 16−24) is 0.21, which is somewhat smaller than those in OG (0.24) and OSE (0.33). The average *f* value of the remaining groups in MEGA-10 (1−15) is 0.66. In general, the values of f_{head} (−▲−) observed for the MEGA-10 head groups are more similar to those of OG and DM than to that of $C_{12}E_8$. This can be understood by noting that the head structure of MEGA-10, like those of OG and DM, contains both hydrogen bond donors and acceptors.

MEGA-10 is difficult to model using the traditional MT modeling approach because it has a hydrophilic nitrogen atom (group 15) surrounded by three hydrophobic groups (CH_2 group 11, CH_3 group 12, and carbonyl groups 13 and 14). A logical starting point for traditional MT modeling would be to identify groups 16−24 as the MEGA-10 tail and to model each of the remaining groups as being part of the MEGA-10 head. By so doing, of course, the approximation is made that all the MEGA-10 head groups (including groups 11−14) remain fully hydrated in the micellar state. The hydration results presented in Figure 9 clearly show that this is indeed an approximation and that, because of their hydrophobic nature and location within the molecule, groups 11−13 are significantly more dehydrated than other hydrophilic or hydrophobic groups in the MEGA-10 head. In Section 4.9, we will compare the CMC predicted by the CS−MT model with the CMC predicted by the traditional MT model and test the assumption that groups 16−24 are part of the MEGA-10 tail.

3.8. Evaluation of Approximations Made in Traditional Molecular-Thermodynamic Modeling. The accuracy of two approximations made in traditional MT modeling to quantify the hydrophobic driving force for micelle formation can be evaluated using the computer simulation data presented above. These include (i) the accuracy of using surfactant head and tail assignments to compute g_{tr} and (ii) the extent to which surfactant heads shield the micelle core from hydrating contacts.

3.8.1. Accuracy of Computing g_{tr} using the Head and Tail Approximation. As discussed in detail in article 1,[1] in traditional MT modeling, the hydrophobic contribution to micelle formation is computed as the sum of two free-energy contributions: the transfer free-energy contribution, g_{tr}, and the interfacial free-energy contribution, g_{int}. A key assumption underlying the traditional MT modeling approach to compute g_{tr} is that the presence of the surfactant head at one end of the surfactant tail does not affect the change in hydration experienced by each group in the surfactant tail as it is transferred from the aqueous solution to a bulk solution of surfactant tails. By making this approximation, g_{tr} may be computed as if the surfactant heads are not present.

However, in practice, changes in the hydration state of the surfactant tail that occur upon its transfer to a bulk phase of tails are affected by the nature of the surfactant head attached

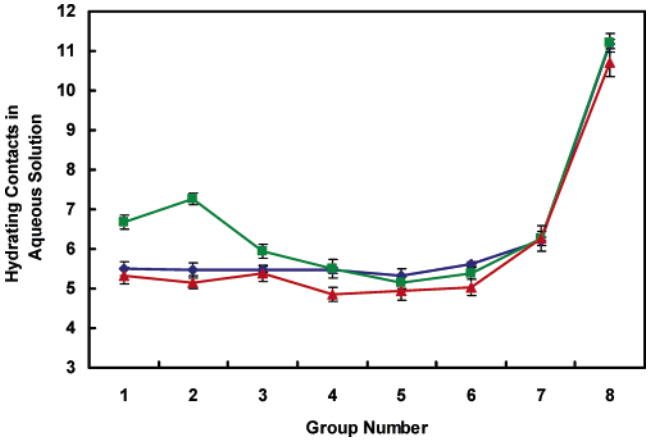

Figure 10. The number of hydrating contacts, as defined in the text, experienced in bulk water for 8 hydrophobic CH_2 or CH_3 groups in hexadecane (−◆−), octyl glucoside (OG, −■−), and octyl sulfinyl ethanol (OSE, −▲−). The first group listed for each surfactant corresponds to the CH_2 group adjacent to the tail's point of attachment to the surfactant head, and the last group listed for all three alkyl chains corresponds to the terminal CH_3 group. The error bars shown correspond to the standard error of the mean.

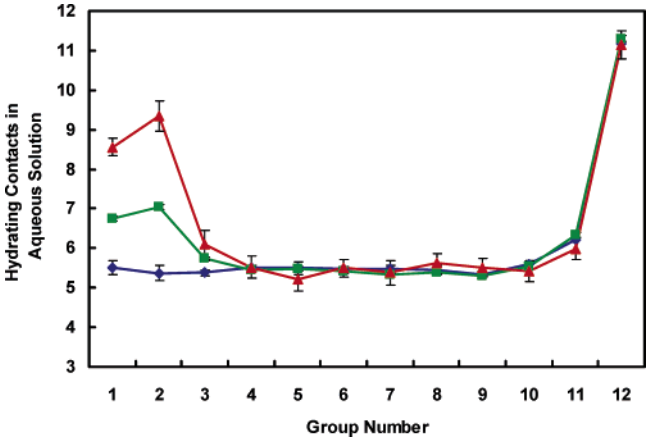

Figure 11. The number of hydrating contacts, as defined in the text, experienced in bulk water for 12 hydrophobic CH_2 or CH_3 groups in hexadecane (−◆−), dodecyl maltoside (DM, −■−), and dodecyl octa-(ethylene oxide) ($C_{12}E_8$, −▲−). The first group listed for each surfactant corresponds to the CH_2 group adjacent to the tail's point of attachment to the surfactant head, and the last group listed for all three alkyl chains corresponds to the terminal CH_3 group. The error bars shown correspond to the standard error of the mean.

to it. This can be shown by comparing hydration data for an oil molecule in bulk water to that of a surfactant tail in bulk water. We have computed the average number of hydrating contacts (as defined in Section 2.4) in bulk aqueous solution for each CH_2 and CH_3 group in hexadecane, as well as for those in the linear alkyl tails of several representative nonionic surfactants with tails containing either 8 or 12 CH_x ($x = 2$ or 3) groups. A cutoff of 0.3 nm was used to define hydrating contacts. In Figure 10, plots of hydrating contacts as a function of group number in the bulk aqueous solution are shown for 8 hexadecane groups (see the −◆− results), the 8 hydrophobic tail groups of OG (−■−), and the 8 hydrophobic tail groups of OSE (−▲−). In Figure 10, group 1 for OG and OSE is defined as the CH_2 group adjacent to the surfactant head, and group 8 for OG, OSE, and hexadecane corresponds to the terminal CH_3 group of each alkyl chain. In Figure 11, plots of hydrating contacts as a function of group number in the bulk aqueous solution are shown for 12 hexadecane groups (−◆−), the 12 hydrophobic tail groups of DM (−■−), and the 12 hydrophobic tail groups of $C_{12}E_8$ (−▲−). In Figure 11, group 1 for the surfactants is defined as the CH_2 group adjacent to the surfactant head, and group 12 for the surfactants and for hexadecane corresponds to the terminal CH_3 group of each alkyl chain. Note that we have not compared the OG and the OSE results with octane hydration data, or the DM and the $C_{12}E_8$ results with dodecane hydration data, because group 1 for each surfactant is a CH_2 group, rather than a CH_3 group. The hydration data presented in Figures 10 and 11 for the surfactants and hexadecane enables us to compare the hydration of chemically identical hydrophobic groups. The error bars shown in Figures 10 and 11 represent standard errors of the mean.

A comparison of the hydration profiles for OG, OSE, DM, and $C_{12}E_8$ with corresponding groups in hexadecane clearly shows that the surfactant head type has an effect on the hydration state of the adjacent CH_2 group in aqueous solution. In addition, our results show that the presence of the surfactant head affects the hydration states of a significant number of hydrophobic groups further down each linear alkyl chain (groups 2 and 3 for OG, DM, and $C_{12}E_8$; groups 2−6 for OSE). The total number of hydrating contacts experienced by groups 1−8 of OG and OSE is 6.3% larger and 5.16% smaller, respectively, than those experienced by the 8 corresponding groups in hexadecane. The total number of hydrating contacts experienced by groups 1−12 of DM and $C_{12}E_8$ is 4.2% larger and 10.1% greater, respectively, than those experienced by the 12 corresponding groups in hexadecane.

Because the extent of hydration of the surfactant tail in the bulk water reference state is affected by the type of surfactant head, it follows that the change in hydration incurred upon transfer of the surfactant tail to a bulk phase of tails is affected by the type of surfactant head. The assumption made in traditional MT modeling in computing g_{tr} that every tail group is dehydrated to the same degree as a tail with no attached head is clearly an approximation.[2,8] Nevertheless, it is important to point out that traditional MT modeling has been shown to yield quantitatively, or semiquantitatively, accurate predictions of the micellization behavior of relatively simple nonionic surfactants.[2,8] Accordingly, the hydration approximations that are made in traditional MT modeling to compute g_{tr} appear reasonable in the absence of detailed hydration data. The CS−MT modeling approach, however, eliminates the need to make such approximations by computing the changes in hydration that occur upon micelle formation directly from molecular dynamics simulation results.

3.8.2. Effect of the Surfactant Heads on Aggregate Core Hydration. The interfacial free-energy contribution, g_{int}, reflects the free-energy penalty associated with forming the micelle core−water interface and is computed in the context of traditional MT modeling using a micelle core−water interfacial tension. Specifically, g_{int} is computed as follows:[1]

$$g_{int} = (a - a_0)\sigma \tag{11}$$

where a is the area per surfactant molecule at the micelle core−water interface, a_0 is the interfacial area that is screened by each surfactant head, and σ is a composition-weighted average of the curvature-corrected interfacial tension between water and a bulk phase of hydrophobic tails (for complete details, see article 1). In our past work, we have estimated a_0 as being equal to 21 Å^2 for every surfactant head in the micelle,[8] an area that is equal to the cross-sectional area of a linear alkyl chain. Nagarajan et al. have modeled a_0 as being equal to the smaller of two areas−

TABLE 2: Evaluation of Traditional MT Modeling Approximations[a]

	N_{cont}	$N_{cont} - N_{cont,oil\ agg}$	shielded area [Å^2]
octane	18.25	0.00	
OG	10.65	−7.61	31.22
OSE	15.28	−2.97	12.19
dodecane	18.97	0.00	
DM	12.14	−6.83	26.99
$C_{12}E_8$	14.66	−4.31	17.03

[a] Simulation results for the number of hydrating contacts (N_{cont}) on a per oil or surfactant molecule basis experienced by octane, octyl glucoside (OG), octyl sulfinyl ethanol (OSE), dodecane, dodecyl maltoside (DM), and dodecyl octa(ethylene oxide) ($C_{12}E_8$) in the aggregate environment. The octane results correspond to the results for a spherical octane aggregate of aggregation number 25.[1] The dodecane results correspond to a spherical dodecane aggregate of aggregation number 33.[1] As described in the text, hydrating contacts results for each micelle have been scaled by the ratio of the micelle core area to the area of either the octane or the dodecane oil aggregate. The change in the number of hydrating contacts relative to the corresponding oil aggregate ($N_{cont} - N_{cont,oil\ agg}$) is also listed, again on a per oil or per surfactant molecule basis. The shielded area reported for the surfactant micelles corresponds to the area at the micelle core−water interface that is effectively shielded from hydrating contacts by the surfactant heads.

the cross-sectional area of a linear alkyl chain (21 Å^2) or the cross-sectional area of the surfactant head.

The curvature-dependent interfacial tension of a surfactant tail of type j in the micelle has been estimated using the Gibbs−Tolman−Koenig−Buff equation:[28−31]

$$\sigma_j = \frac{\sigma_{0,j}}{\left(1 + \frac{(S-1)\delta}{l_c}\right)} \tag{12}$$

where $\sigma_{0,j}$ is the interfacial tension of component j at a flat interface with water (typically around 50 mN/m for hydrocarbons), δ is the Tolman distance, and S is a shape factor that is equal to 3 for spheres, 2 for cylinders, and 1 for disks or bilayers. The estimation of $\sigma_{0,j}$ for alkyl chains of varying length and as a function of temperature, as well as the estimation of the Tolman distance, δ, were discussed in detail in article 1.[1]

The simulation data reported in Sections 3.1−3.7 can be used to evaluate how physically reasonable eq 11 is as implemented in the context of the traditional MT modeling approach. By comparing simulation results for the small spherical octane aggregate (see article 1)[1] with those for the OG and the OSE micelles, as well as simulation results for the large spherical dodecane aggregate[1] with those for the DM and the $C_{12}E_8$ micelles, it is possible to comment on the extent to which the surfactant heads shield the micelle hydrophobic core from hydrating contacts. These two oil aggregates have been selected for comparison because their surface areas are similar to those of the simulated micelles. Table 2 reports the total number of hydrating contacts, N_{cont}, for octane, OG, OSE, dodecane, DM, and $C_{12}E_8$ in the aggregate state on a per molecule basis. To allow direct comparison of the results for the oil aggregates and for the micelles, N_{cont} for OG and OSE were computed by scaling the OG and the OSE hydrating contact results by ($A_{core,mic}/A_{core,oct\ agg}$), where $A_{core,mic}$ is the surface area of the surfactant micelle core and $A_{core,oct\ agg}$ is the surface area of the octane aggregate, to correct for differences in aggregate surface area. We consider scaling based on surface area to be appropriate because hydrating contacts should be approximately proportional to the exposed surface area. Similarly, N_{cont} for DM and $C_{12}E_8$ was computed by scaling the DM and the $C_{12}E_8$ hydrating contact results by ($A_{core,mic}/A_{core,dod\ agg}$), where $A_{core,dod\ agg}$ is the surface area of the dodecane aggregate. Table 2 also reports the difference between the number of hydrating contacts for OG or OSE and the number of hydrating contacts for octane, as well as the difference between the number of hydrating contacts for DM or $C_{12}E_8$ and the number of hydrating contacts for dodecane as ($N_{cont} - N_{cont,oil\ agg}$). The decrease in the number of hydrating contacts observed for each surfactant micelle relative to the corresponding value for each oil aggregate can be used to infer the area at the micelle core−water interface that is effectively shielded from hydrating contacts by the surfactant heads. These results are reported in Table 2 as the "shielded area" values. The average of these shielded area values (21.85 Å^2) is very similar to the shielded area value used in traditional MT modeling (21 Å^2). However, inspection of the shielded area results reveals that the shielded area varies significantly among the surfactants considered. The shielded area calculated for OSE, for example, at 12.19 Å^2, is less than half of the shielded area calculated for OG (31.22 Å^2). An advantage of the CS−MT modeling approach is that it permits estimation of the hydrophobic contribution to g_{form} (as reflected in $g_{dehydr} + g_{hydr}$) without making any assumptions about the effect of the surfactant heads on the hydration state of the micelle core.

4. Molecular-Thermodynamic Modeling Based on Computer Simulation Inputs

4.1. Using the CS−MT Modeling Approach to Predict Surfactant Micellization Behavior. As stressed in article 1, using the CS−MT modeling approach to quantify the hydrophobic effect for oil aggregates in water is less challenging than using it to model surfactant micellization. Indeed, in surfactant micellization, the presence of the surfactant heads at the aggregate core−water interface introduces several complications that are absent in the oil aggregate case. To deal with these complications, we will make a number of simplifying approximations. Following a description of these approximations in Sections 4.1.1 and 4.1.2, we will use the CS−MT model to predict g_{form} and the CMC for each of the seven nonionic surfactants discussed in Section 3. Although the CS−MT model enables the prediction of a variety of micellar solution properties from g_{form} (including micelle shape, size, and composition), the surfactant CMC was selected for prediction and comparison with experimental CMC data because the CMC depends exponentially on g_{form}, and as such, it provides a stringent quantitative test with which to evaluate the predictive accuracy of the CS−MT model. The CMCs predicted by the CS−MT model will be compared both with the CMCs predicted by the traditional MT model and with the experimental CMC values. In addition, the accuracy of the approximations made in implementing the CS−MT model will be discussed in the context of the CS−MT and the traditional MT modeling results.

4.1.1. Estimation of g_{dehydr}. When using the CS−MT model to quantify the hydrophobic effect, eq 2 is used for every hydrophobic group in the surfactant molecule, regardless of whether the hydrophobic group is part of the surfactant head or the surfactant tail. Accordingly, every hydrophobic group in the surfactant molecule contributes to the hydrophobic driving force for micelle formation to the extent that the group is dehydrated upon micelle formation. To implement eq 2, therefore, suitable values of g_{tr_i} must be estimated for every hydrophobic group in the surfactant molecule.

In traditional MT modeling, only the surfactant tails are considered to be dehydrated upon micelle formation. In that case, the transfer free-energy contribution, g_{tr}, of these tails can

be estimated in a straightforward manner using experimental tail solubility data, or a theoretical estimate of tail solubility can be made using a group-contribution approach (see article 1 for a detailed discussion).[1] Similarly, in CS−MT modeling, g_{tr_i} values of hydrophobic groups in the surfactant tail can be determined from an estimate of the solubility of group *i* in water. Suitable g_{tr_i} values of hydrophobic groups in the surfactant head are more difficult to estimate. Dehydration of the surfactant heads upon micelle formation may result from solvent exclusion by other surfactant heads, contact with hydrophobic groups in other surfactant heads, and contact with the micelle hydrophobic core. Due to the highly anisotropic nature of the micelle core−water interfacial region, it is difficult to assign suitable g_{tr_i} values associated with transfer from bulk water to this interfacial environment because the required experimental solubility data is not available. To the best of our knowledge, there are no simple theoretical approaches to predict g_{tr_i} between bulk water and such a complex, anisotropic environment. A second complication in estimating g_{tr_i} values for groups in the surfactant head results from the fact that the hydrophobicity of hydrophobic groups in the surfactant head may be affected by their being bonded to hydrophilic groups. In molecular mechanics force fields, the chemical effect of being bonded to a hydrophilic group is captured by the fact that the atomic charge of each atom in a molecule is a function of its adjacent atoms.[11] For example, in the OPLS-AA force field, the net atomic charge assigned to the CH_2 group in poly(ethylene oxide) is 0.1 | *e* | (where *e* is the charge of an electron), which differs from the net charge of 0 | *e* | assigned to a CH_2 group bonded to alkyl groups.

With the above complications in mind, in order to implement the CS−MT model in a straightforward manner, in this article, we make the approximation that the g_{tr_i} values of hydrophobic groups in the surfactant head are identical to the g_{tr_i} values of the same hydrophobic groups in the surfactant tail. We anticipate that implementing the CS−MT model in this approximate way should yield an improvement over the traditional MT modeling approach for many surfactants. In the traditional MT modeling approach, hydrophobic groups in the surfactant head do not contribute at all to the hydrophobic driving force for micelle formation. However, it is important to note that obtaining better estimates of g_{tr_i} for hydrophobic groups in the surfactant head represents an important area for future research in order to improve the accuracy of the CS−MT model.

For the seven nonionic surfactants modeled here, we only need to consider CH, CH_2, and CH_3 hydrophobic groups. Accordingly, to implement the CS−MT model, g_{tr_i} values for CH_2 and CH_3 were estimated using the same solubility correlations for linear alkyl tails that are used in traditional MT modeling.[32] The g_{tr_i} value for CH was estimated using solubility data for branched alkyl tails.[33]

4.1.2. Estimation of g_{hydr}. In article 1, we presented an approach to theoretically estimate g_{hydr} for oil molecules. In our model for g_{hydr}, we calculated Δg_{wc} using eqs 5 and 6. In estimating g_{hydr} for each of the hydrophobic groups in a surfactant molecule, two complications arise: (i) g_{hydr} is nonzero only for those hydrophobic groups in the surfactant molecule that are adsorbed onto, or that penetrate into, the micelle hydrophobic core, and (ii) for those hydrophobic groups that are adsorbed onto, or that penetrate into, the micelle hydrophobic core, Δg_{wc} may be affected by the presence of the surfactant heads at the micelle core−water interface.

Note that the free-energy contribution, g_{hydr}, is zero for those hydrophobic groups that are not part of the micelle hydrophobic core, because g_{hydr} accounts for the difference in free energy associated with hydrating contacts in the bulk water and in the aggregate environment. Fundamentally, the origin of g_{hydr} is the size dependence of hydration thermodynamics. An isolated hydrophobic chain in water is much smaller in size than a typical aggregate core−water interface. Therefore, the hydrophobic chain disrupts the hydrogen-bonding and coordinate-bonding network of the aqueous solution to a different extent. Hydrophobic groups in a surfactant molecule that are not part of the micelle hydrophobic core continue to disrupt this hydrogen-bonding and coordinate-bonding network in the aggregate state in much the same way that they do in the bulk water state. Consequently, g_{hydr} for such groups is zero. With this in mind, we will consider any hydrophobic group that has an *f* value equal to, or less than, 0.60 to be part of the micelle hydrophobic core (see below) and to have a nonzero value of g_{hydr}.

The selection of $f = 0.60$ as the appropriate cutoff value was motivated both by physical intuition and by our computer simulation results. For a hydrophobic group located precisely at a flat oil−water interface (with half of its surface in oil and the other half in water), the average value of *f* computed through molecular dynamics simulation would be 0.5. For a hydrophobic group adsorbed at a curved, rough oil−water interface, we would expect the average value of *f* to be greater than 0.5. We note that, for the small, spherical hexadecane oil aggregate simulated in article 1, the average value of *f* for the two terminal CH_3 groups was found to be 0.53, even though each of the CH_3 and the CH_2 groups in the hexadecane molecules are part of the aggregate core. We selected $f = 0.6$ as a suitable cutoff value after considering simulation results for the seven nonionic surfactants modeled here, as well as simulation results for a number of simple, ionic surfactants, including sodium dodecyl sulfate (SDS), cetyltrimethylammonium bromide (CTAB), and decyltrimethylammonium bromide (DTAB). CS−MT modeling results for these three ionic surfactants will be presented in article 3 of this series.[34] For each of the nonionic and ionic surfactants that we simulated, groups that would be considered to be part of the surfactant head in traditional MT modeling had an *f* value greater than 0.60, and groups that would be considered to be part of the surfactant tail in traditional MT modeling had an *f* value that is less than, or equal to, 0.60. In traditional MT modeling, all the atoms in the surfactant tail are considered to be part of the micelle core, and such an assignment yields quantitatively, or semiquantitatively, accurate predictions of the micellar solution behavior of simple surfactants.[8] In this article, therefore, we treat any hydrophobic groups in a surfactant molecule with an *f* value that is less than, or equal to, 0.60 as being part of the micelle hydrophobic core.

For those hydrophobic groups that are identified as being part of the micelle hydrophobic core, a reasonable value of Δg_{wc} must be estimated in order to compute g_{hydr} using eq 4. We propose that, to a first approximation, Δg_{wc} can be evaluated as being equal to the value calculated for oil molecules in article 1.[1] As shown in eq 5, Δg_{wc} is the difference between the free energy per unit SASA in the aggregate core state (σ_{core}) and in the bulk water state (σ_{bulk}). The value of σ_{bulk} for a hydrophobic group in a surfactant molecule is very similar to that of σ_{bulk} for a hydrophobic group in an oil molecule. Furthermore, the success of the traditional MT approach in modeling the aggregate core−water interface using an oil−water interfacial tension[1] indicates that assuming that σ_{core} in a micelle is equal to σ_{core} of an oil−water interface is a reasonable approximation. This approximation has been made in modeling each of the

TABLE 3: Modeling Results for the Simulated Micelles[a]

surfactant	g_{dehydr} [k_BT]	g_{hydr} [k_BT]	$\hat{g}_{int}$ [k_BT]	$g_{tr,CS-MT}$ [k_BT]	g_{tr} [k_BT]
OG	-12.11 ± 0.06	1.51 ± 0.02	4.01	-14.61 ± 0.06	-13.98
DM	-17.90 ± 0.05	2.25 ± 0.02	4.71	-20.36 ± 0.06	-20.06
OSE	-10.53 ± 0.10	1.31 ± 0.02	4.34	-13.55 ± 0.10	-13.98
$C_{10}PO$	-14.34 ± 0.05	1.44 ± 0.03	3.86	-16.75 ± 0.06	-16.96
$C_{10}SO$	-13.08 ± 0.12	1.38 ± 0.04	3.86	-15.56 ± 0.12	-16.96
$C_{12}E_8$, all hydr groups	-21.04 ± 0.22	1.29 ± 0.06	4.90	-24.65 ± 0.23	-19.95
$C_{12}E_8$, tail hydr groups	-16.76 ± 0.09	0.55 ± 0.05	4.90	-21.10 ± 0.10	-19.95
MEGA$-$10	-14.91 ± 0.16	1.36 ± 0.06	3.81	-17.36 ± 0.17	-15.47

[a] CS$-$MT and traditional MT modeling results for each of the seven simulated nonionic surfactant micelles considered in this article. CS$-$MT model predictions of g_{dehydr}, g_{hydr}, $\hat{g}_{int}$, and $g_{tr,CS-MT}$ were made as described in Section 1.1. The uncertainties reported for the CS$-$MT model predictions correspond to the standard error of the mean. Traditional MT modeling results for g_{tr} are presented for comparison with $g_{tr,CS-MT}$. For $C_{12}E_8$, CS$-$MT modeling results generated by summing in eq 2 over all the hydrophobic (hydr) groups in the $C_{12}E_8$ molecule, as well as over only the $C_{12}E_8$ tail hydrophobic (hydr) groups, are reported separately (see Section 4.8).

TABLE 4: Modeling Results for the Optimal Micelles[a]

surfactant	shape	n	g_{int} [k_BT]	g_{pack} [k_BT]	g_{st} [k_BT]	g_{form} [k_BT] (CMC [mM]) CS$-$MT model	MT model	experimental
OG	cyl	43	3.23	2.17	1.54	-8.67 ± 0.06 (9.52 ± 0.57)	-8.04 (17.97)	-7.74 (24.1)
DM	cyl	58	4.31	2.23	1.91	-12.89 ± 0.06 (0.14 ± 0.01)	-12.60 (0.19)	-12.87 (0.14)
OSE	cyl	535	2.71	2.39	1.07	-8.39 ± 0.10 (12.59 ± 1.27)	-8.81 (8.26)	-7.62 (27)
$C_{10}PO$	cyl	45	4.08	2.16	1.87	-9.64 ± 0.06 (3.61 ± 0.23)	-9.85 (2.93)	-9.58 (3.8)
$C_{10}SO$	cyl	12802	2.94	2.50	1.0	-10.13 ± 0.12 (2.23 ± 0.28)	-11.53 (0.54)	-10.38 (1.7)
$C_{12}E_8$	cyl	54	4.41	2.23	1.95	all hydr groups -17.06 ± 0.23 (0.002 ± 0.0) tail hydr groups -13.51 ± 0.10 (0.08 ± 0.01)	-12.36 (0.24)	-13.22 (0.1)
MEGA$-$10	sph	22	4.96	2.39	1.97	-9.05 ± 0.17 (6.55 ± 1.15)	-8.12 (43.33)	-9.31 ± 0.01 (5 ± 0.05)

[a] CS$-$MT and traditional MT modeling results for each of the seven nonionic surfactants considered in this article. Both the CS$-$MT model and the traditional MT model yield identical predictions for the optimal micelle shape, the number-average aggregation number (n), g_{int}, g_{pack}, and g_{st} (see Section 4.2). The CS$-$MT and the traditional MT model predictions of g_{form} were obtained using the values of $g_{tr,CS-MT}$ and g_{tr} reported in Table 3, respectively, as an input to eq 8. The CS$-$MT and the traditional MT model predictions of the CMC and the value of g_{form} inferred using the experimental CMC data were calculated using eq 9. The uncertainties reported for the CS$-$MT model predictions correspond to the standard error of the mean. For $C_{12}E_8$, CS$-$MT modeling results generated by summing in eq 2 over all the hydrophobic (hydr) groups in the $C_{12}E_8$ molecule, as well as over only the $C_{12}E_8$ tail hydrophobic (hydr) groups, are reported separately (see Section 4.8).

seven nonionic surfactants considered in this article, which we discuss below.

4.2. Modeling Results for Octyl Glucoside (OG). Using the simplifying approximations discussed in Sections 4.1.1 and 4.1.2, we used the CS$-$MT model to predict the micellization behavior for OG in aqueous solution at 25 °C. In Table 3, we report CS$-$MT modeling results for the *simulated* OG micelle, including (i) g_{dehydr}, (ii) g_{hydr}, (iii) $\hat{g}_{int}$, and (iv) $g_{tr,CS-MT}$. The reported uncertainty for the CS$-$MT modeling results corresponds to the standard error of the mean, as computed through block averaging. The CS$-$MT modeling results for g_{dehydr} and g_{hydr} were generated using f values, which, as discussed in Section 3.1, are based on contacts with water and with hydrogen-bonding groups in the surfactant head. The value of g_{dehydr} ($-12.11k_BT$) is much larger in magnitude than that of g_{hydr} ($1.51k_BT$). The physical interpretation of this result is that the free-energy contribution associated with the dehydration of each group in OG is significantly larger in magnitude than the free-energy contribution arising from the difference in free energy associated with hydration in the micellar state and in the bulk aqueous solution (or, in other words, the free-energy contribution arising from the size dependence of hydration thermodynamics discussed in Section 3.4 in article 1). However, as shown in Table 4 (see below), if g_{hydr} is not included in the CS$-$MT model, accurate CS$-$MT modeling results would not be obtained. Equation 7 was used to compute $g_{tr,CS-MT}$ from g_{dehydr}, g_{hydr}, and $\hat{g}_{int}$. In Table 3, we also report the traditional MT model prediction of g_{tr} for comparison with $g_{tr,CS-MT}$. We note that the CS$-$MT model prediction for the transfer free-energy contribution ($g_{tr,CS-MT} = -14.61k_BT$) is $0.63k_BT$ more negative than the traditional MT model prediction ($g_{tr} = -13.98k_BT$).

In Table 4, we report CS$-$MT and traditional MT modeling results for micelles of the optimal shape and size. The optimal micelle shape and size are predicted to be the values that minimize g_{form}.[8] Although the CS$-$MT model predicts a different g_{form} value than that obtained using the traditional MT model, both models yield identical predictions for the optimal micelle shape and size. This equivalence arises because the only contribution to g_{form} that differs in the two models (the transfer free-energy contribution) does not depend on the micelle shape and size and therefore does not affect the minimization procedure used to determine the optimal micelle properties. As discussed in Section 2.3, the computer simulation of the OG micelles was conducted for a spherical micelle with an aggregation number of 29, but both the CS$-$MT model and the traditional MT model predict that the optimal micelles are cylindrical with a number-average micelle aggregation number of 43. In Table 4, we report predictions of the CS$-$MT model and the traditional MT model for (i) the optimal micelle shape, (ii) the number-average aggregation number (n), (iii) g_{int}, (iv) g_{pack}, (iv) g_{st}, (v) the CS$-$MT model predictions of g_{form} and the CMC, (vi) the traditional MT model predictions of g_{form} and the CMC, and (vii) the experimental values of g_{form} and the CMC.[35] The reported uncertainty for the CS$-$MT modeling results is the standard error of the mean, as computed through block averaging. The CS$-$MT and the traditional MT model predictions for g_{form} were obtained by using $g_{tr,CS-MT}$ and g_{tr}, respectively, as an input to eq 8. In applying the CS$-$MT model

and the traditional MT model, the surfactant head area, a_h, was modeled as being equal to 40 Å^2.[8] Note that the molecular parameter, a_h, is used to calculate the steric free-energy contribution, g_{st}.[8,36] Traditional MT modeling results were generated using the traditional MT modeling approach reviewed in article 1.[1] In generating the traditional MT modeling results, each OG surfactant was modeled as having 7 CH_2 groups and 1 CH_3 group in the surfactant tail (groups 13−20 in Figure 3). The CS−MT and the traditional MT model predictions of the CMC and the value of g_{form} inferred using the experimental CMC data were calculated using eq 9.

Because the shape and size of the optimal micelles predicted by the CS−MT model and the traditional MT model are identical, the values of g_{int}, g_{pack}, and g_{st} predicted by each model are also identical.[8] Although the predicted value of g_{int} is the same in both the CS−MT model and the traditional MT model, as shown in Tables 3 and 4, the value of g_{int} computed for the optimal micelle ($3.23k_BT$) is significantly lower than the value of $\hat{g}_{int}$ computed for the simulated micelle ($4.01k_BT$). The free-energy contributions, g_{st} ($1.54k_BT$) and g_{pack} ($2.17k_BT$), although smaller than g_{int}, both contribute significantly to g_{form}. Values of g_{ent} and g_{elec} are not reported because they are equal to zero for this nonionic, single-surfactant system. The CS−MT model, the MT model, and the experimental values of g_{form} are all within $0.63k_BT$ of each other. The CS−MT and the traditional MT model predictions of the CMC, as well as the value of g_{form} inferred using the experimental CMC data, were calculated using eq 9. Both the CS−MT model and the traditional MT model predict CMC values that are somewhat lower than the experimental CMC value of 24.1 mM.[35] The CMC predicted by the CS−MT model is 61% lower than the experimental CMC value, and the CMC predicted by the traditional MT model is 25% lower than the experimental CMC value. This discrepancy reflects the different estimates of the hydrophobic driving force for micelle formation obtained using the two models ($g_{tr,CS-MT}$ and g_{tr}, as reported in Table 3). Although the traditional MT model result for the CMC is closer to the experimental CMC value than the CS−MT result for the CMC, we consider both the CS−MT model and the traditional MT model CMC predictions shown in Table 3 to be in reasonable agreement with the experimental data, given the exponential dependence of the CMC on g_{form} (see eq 9).

4.3. Modeling Results for Dodecyl Maltoside (DM). CS−MT modeling results for the simulated DM micelle are reported in Table 3, where each free-energy contribution was calculated as described in Section 4.2. Theoretical predictions for the optimal micelles obtained using the CS−MT model and the traditional MT model, as well as the experimental data[37] for the micellization behavior of DM in aqueous solution at 25 °C with 0.1 M of added NaCl, are reported in Table 4. The approach described in Section 4.2 was used to calculate each free-energy contribution, the g_{form} values, and the CMC values. In using the CS−MT model and the traditional MT model, the surfactant head area, a_h, was modeled as being equal to 52 Å^2.[8]

Although computer simulation of DM was conducted in a micelle with an aggregation number of 45, the optimal DM micelles that are predicted to form in solution by the CS−MT model and the traditional MT model are small cylinders with a number-average aggregation number of 58. The predicted value of g_{int} ($4.31k_BT$) is slightly lower than that of $\hat{g}_{int}$ ($4.71k_BT$) due to this aggregation number difference. The predicted value of g_{st} is slightly larger for the optimal DM micelle ($1.91k_BT$) than the predicted value for the optimal OG micelle ($1.54k_BT$), because the DM head (groups 1−23) is modeled as being 12 Å^2 larger in cross-sectional area than the OG head (groups 1−12).[8] As in OG, the CS−MT model prediction of the transfer free-energy contribution ($g_{tr,CS-MT} = -20.36k_BT$) is slightly more negative than that of the traditional MT model prediction ($g_{tr} = -20.06k_BT$). This leads to the CS−MT model predicting a lower CMC (0.14 mM) than that predicted by the traditional MT model (0.19 mM). In this case, the CS−MT model prediction of the CMC agrees remarkably well with the experimental value (0.14 mM).

4.4. Modeling Results for Octyl Sulfinyl Ethanol (OSE). CS−MT modeling results for the simulated OSE micelle are reported in Table 3, where each free-energy contribution was calculated as described in Section 4.2. Theoretical predictions for the optimal micelles obtained using the CS−MT model and the traditional MT model, as well as the experimental data[38] for the micellization behavior of OSE in aqueous solution at 25 °C, are reported in Table 4. The approach described in Section 4.2 was used to calculate each free-energy contribution, the g_{form} values, and the CMC values listed in Table 4. In applying the CS−MT model and the traditional MT model, the surfactant head area, a_h, was modeled as being equal to 30 Å^2.[8]

Although computer simulation of an OSE micelle was conducted at an aggregation number of 25, the optimal OSE micelles that are predicted using the CS−MT model are cylinders with a number-average aggregation number of 535. The predicted value of g_{int} ($2.71k_BT$) is significantly lower than that of $\hat{g}_{int}$ ($4.34k_BT$) due to this large aggregation number difference. The g_{int} value for OSE is $1.60k_BT$ lower than that for DM and $0.52k_BT$ lower than that for OG due to the large aggregation number of the OSE micelle, which lowers the interfacial area per surfactant molecule.[8] For OSE, $g_{tr,CS-MT}$ ($-13.55k_BT$) is slightly less negative than g_{tr} computed using the traditional MT modeling approach ($-13.98k_BT$). As a result, the CS−MT model prediction of the CMC is higher than the MT model prediction of the CMC, and it is also slightly closer to the experimental CMC value. As shown in Figure 5, groups 2 and 3 in OSE both have relatively high f values. However, the net effect of using eqs 2 and 4 to determine the contribution of both of these groups to the hydrophobic driving force for micelle formation is still significant, at $-0.71k_BT$. Allowing all the hydrophobic groups in the surfactant molecule (and not just those in the surfactant tail) to contribute to g_{form} shifts the CS−MT model prediction of the CMC for OSE closer to the experimental CMC value.

4.5. Modeling Results for Decyl Dimethyl Phosphine Oxide (C_{10}PO). CS−MT modeling results for the simulated C_{10}PO micelle are reported in Table 3. Theoretical predictions for the optimal micelles obtained using the CS−MT model and the traditional MT model, as well as the experimental data[39] for the micellization behavior of C_{10}PO in aqueous solution at 24 °C with 0.1 mM of added Na_2CO_3, are reported in Table 4. All the free-energy contributions, the g_{form} values, and the CMC values listed in Tables 3 and 4 were computed using the approach described in Section 4.2. In applying the CS−MT model and the traditional MT model, the surfactant head area, a_h, was modeled as being equal to 50 Å^2.[8]

Although computer simulation of C_{10}PO was done in a micelle with an aggregation number of 50, the optimal micelles predicted by the CS−MT model and the traditional MT model are small cylindrical micelles with a number-average aggregation number of 45. The predicted value of g_{int} ($4.08k_BT$) is slightly higher than that of $\hat{g}_{int}$ ($3.86k_BT$) because the optimal micelle is predicted to have a slightly larger aggregation number than that of the simulated micelle. For this surfactant, the predictions of

the CS−MT model and the traditional MT model for g_{form} and the CMC are quite similar. Our estimate of $g_{tr,CS-MT}$ ($-16.75k_BT$) is only $0.21k_BT$ less negative than our estimate of g_{tr} ($-16.96k_BT$), but nevertheless, this leads to a CMC prediction that is closer to the experimental CMC value than the CMC predicted using traditional MT modeling. In the CS−MT model, it is interesting to note that, despite their high f values, groups 1 and 2 (as defined in Figure 6) contribute a total of $-0.65k_BT$ to the hydrophobic driving force for micelle formation. Despite this negative free-energy contribution from the $C_{10}PO$ head, the CMC predicted by the CS−MT model is higher than the CMC predicted by the MT model. This can be explained by the fact that the CS−MT modeling approach models the hydration of the surfactant tail and its contribution to $g_{tr,CS-MT}$ in a different manner than the traditional MT model.

4.6. Modeling Results for Decyl Methyl Sulfoxide ($C_{10}SO$). CS−MT modeling results for the simulated $C_{10}SO$ micelle are reported in Table 3. Theoretical predictions for the optimal micelles obtained using the CS−MT model, as well as the traditional MT model and the experimental data[39] for the micellization behavior of $C_{10}SO$ in aqueous solution at 24 °C with 0.1 mM of added Na_2CO_3, are reported in Table 4. The results reported in Tables 3 and 4 for $C_{10}SO$ were computed using the approach described in Section 4.2. In applying the CS−MT model and the traditional MT model, the surfactant head area, a_h, was modeled as being equal to 30 Å^2.[8]

Like $C_{10}PO$, the $C_{10}SO$ micelle was simulated with an aggregation number of 50. However, the CS−MT model prediction for the optimal aggregation number was found to correspond to large cylindrical micelles with a number-average aggregation number of 12 802. The predicted value of g_{int} for $C_{10}SO$ ($2.94k_BT$) is significantly lower than the predicted value of g_{int} for $C_{10}PO$ ($4.08k_BT$). For $C_{10}SO$, the CS−MT model estimate of $g_{tr,CS-MT}$ ($-15.56k_BT$) is $1.4k_BT$ larger than the traditional MT model estimate of g_{tr} ($-16.96k_BT$), making the CS−MT model estimate of the CMC significantly larger than that of the traditional MT model and closer to the experimental CMC value. Group 1 of $C_{10}SO$ (see Figure 7) contributes $-0.66k_BT$ to $g_{tr,CS-MT}$, but the overall hydrophobic driving force for micelle formation is predicted to be higher using the CS−MT model than using the traditional MT model. In the next section, the CMC predicted by the CS−MT model and the traditional MT model for binary mixtures of $C_{10}PO$ and $C_{10}SO$ will be presented, and the similarities and differences between the various free-energy contributions to g_{form} for these two surfactants will be discussed in greater detail.

4.7. Modeling Results for Binary Mixtures of $C_{10}PO$ and $C_{10}SO$. In Figure 12, we present both CS−MT model predictions (see the — results) and traditional MT model predictions (- - -) for CMCs of binary mixtures of $C_{10}PO$ and $C_{10}SO$ in aqueous solution at 24 °C with 0.1 mM of added Na_2CO_3. Experimental mixture CMC data (◆) is presented for comparison.[39] CMC values are reported in mM on the y-axis, and the mole fraction of $C_{10}PO$ is reported on the x-axis. The mixture CMC values increase monotonically as the mole fraction of $C_{10}PO$ is increased. Both the CS−MT model and the traditional MT model capture this increase and yield reasonable estimates of the slope associated with this increase. However, the CMCs predicted by the CS−MT model are clearly in better agreement with the experimental CMC values than the CMCs predicted by the traditional MT model.

It is instructive to compare each of the free-energy contributions to g_{form} for $C_{10}PO$ and $C_{10}SO$, as estimated using the CS−MT model and the traditional MT model (see Tables 3 and 4).

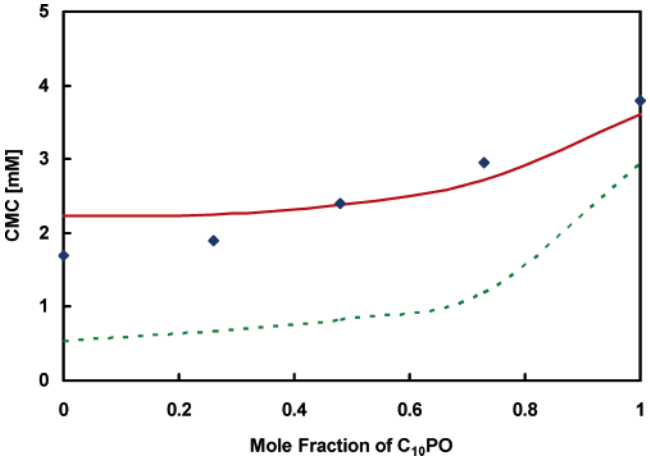

Figure 12. Predicted (— and - - -) and experimental (◆) CMCs of mixtures of $C_{10}PO$ and $C_{10}SO$, where the full line corresponds to CMCs predicted by the CS−MT model and the dashed line corresponds to CMCs predicted by the traditional MT model.

The discrepancy between predictions made using the CS−MT model and the traditional MT model can be explained in terms of the difference between the CS−MT model estimates of $g_{tr,CS-MT}$ and the traditional MT model estimates of g_{tr} for these two surfactants (see Table 3). For $C_{10}PO$, $g_{tr,CS-MT} = -16.75k_BT$ and $g_{tr} = -16.96k_BT$; for $C_{10}SO$, $g_{tr,CS-MT} = -15.56k_BT$ and $g_{tr} = -16.96k_BT$. As can be seen, the traditional MT model predictions for g_{tr} are the same for both $C_{10}PO$ and $C_{10}SO$, because both surfactants have the same number of hydrophobic groups in their tails. The CS−MT model predictions for the transfer free-energy contribution are less negative than those of the traditional MT model, making the CMC predicted using the CS−MT modeling approach higher for both surfactants and closer to the experimental CMC values (see Table 4).

Although the CS−MT model yields more accurate CMC predictions than the traditional MT model for $C_{10}PO$ and $C_{10}SO$, both the CS−MT model and the traditional MT model correctly predict that $C_{10}PO$ has a higher CMC than $C_{10}SO$. In the traditional MT model, the only molecular difference between $C_{10}PO$ and $C_{10}SO$ is their different head sizes (as captured in a_h). Therefore, the physical origin of the difference in CMC predictions for $C_{10}PO$ and $C_{10}SO$ made by the traditional MT model is due to steric effects (g_{st}). However, because the various free-energy contributions are coupled through the minimization of g_{form}, the influence of these steric effects is also manifested in the predicted values of g_{int} and g_{pack}. In the CS−MT modeling approach, the predicted CMCs also differ because of the different $g_{tr,CS-MT}$ values of $C_{10}PO$ and $C_{10}SO$. The steric effects arising from differences in head size, however, more than compensate for the more negative $g_{tr,CS-MT}$ value of $C_{10}PO$ ($-16.75k_BT$) relative to that of $C_{10}SO$ ($-15.56k_BT$) predicted using the CS−MT model, making the predicted CMC of $C_{10}PO$ 1.38 mM higher than that of $C_{10}SO$. In traditional MT modeling, g_{tr} for both surfactants is predicted to be the same, and therefore, the predicted CMC of $C_{10}PO$ is 2.39 mM larger than the predicted CMC of $C_{10}SO$. The experimental CMC difference for these two surfactants is 2.1 mM, which is closer to the CS−MT model prediction for the difference in the CMCs than to the traditional MT prediction for the difference in the CMCs.

4.8. Modeling Results for Dodecyl Octa(Ethylene Oxide) ($C_{12}E_8$). CS−MT modeling results for the simulated $C_{12}E_8$ micelle are reported in Table 3. Theoretical predictions for the optimal micelles obtained using the CS−MT model and the

traditional MT model, as well as the experimental data[40] for the micellization behavior of $C_{12}E_8$ in aqueous solution at 25 °C, are reported in Table 4. The same computational approach described in Section 4.2 was used to generate each of the free-energy contributions to g_{form} and the CMC values listed in Table 3, although for this surfactant, the CS−MT model predictions were made using two different approaches. In the first approach, reported under the heading "all hydr groups" in Table 3, the CS−MT model for g_{dehydr} (given in eq 2) was used to compute the free-energy contribution of every hydrophobic group in the surfactant molecule, regardless of whether the group is part of the surfactant head or tail. This is the modeling approach that has been used to model each of the other nonionic surfactants considered in this article. However, we also implemented CS−MT modeling of $C_{12}E_8$ in an alternate way, reported under the heading "tail hydr groups" in Table 3. In this alternate approach, only the hydrophobic groups in the surfactant tail (i.e., groups 26−37 listed in Figure 8) are included in the sum given in eq 2 to calculate g_{dehydr}. In both implementations of the CS−MT model, as well as in the implementation of the traditional MT model, the surfactant head area, a_h, was modeled as being equal to 53 Å^2.[8]

$C_{12}E_8$ differs from the other six nonionic surfactants considered in this article in that the traditional MT model CMC prediction (0.24 mM) and the experimental CMC (0.1 mM) are in reasonable agreement, but the "all hydr groups" CS−MT modeling approach severely underestimates the CMC (0.002 mM). The regular CS−MT modeling approach fails in this case because of the simplistic manner in which we have used eq 2 for $C_{12}E_8$. As discussed in Section 4.2, the values of g_{tr_i} used in eq 2 are strictly accurate only for the transfer of a hydrophobic oil group (CH, CH_2, or CH_3) from bulk water to a bulk phase of tails. For eq 2 to yield reasonable results, an accurate estimate of g_{tr_i} must first be made for each of the CH_2 groups in the E_8 head of $C_{12}E_8$. As discussed in Section 4.1, we have made the approximation that, for each of the nonionic surfactants modeled here, the g_{tr_i} values corresponding to hydrophobic groups in the surfactant head are equal to the g_{tr_i} values for the corresponding groups in the surfactant tail. For $C_{12}E_8$, however, we believe that this approximation is not sufficiently accurate for the following reasons: (i) using a water-to-oil transfer free energy for the process of transferring a CH_2 group in E_8 from bulk water to the corona region of a $C_{12}E_8$ micelle (which has a high concentration of water and other ethylene oxide groups) is a poor approximation, (ii) each of the hydrophobic groups in the surfactant head is bonded to a hydrophilic oxygen atom, thus affecting its hydrophobicity and g_{tr_i} value, and (iii) the large number of hydrophobic groups in the E_8 head (a total of 16) amplifies the effect of errors inherent in (i) and (ii) to a greater extent than that observed in the case of the other six nonionic surfactants considered in this article, which have relatively small, non-polymeric heads.

The CS−MT model tail hydr groups approach actually yields the most accurate prediction of the CMC when compared with the experimental CMC. Clearly, for $C_{12}E_8$, approximating each of the hydrophobic groups in the E_8 head of $C_{12}E_8$ as not contributing at all to the hydrophobic driving force for micelle formation is more appropriate than modeling them as contributing to the hydrophobic driving force with the same g_{tr_i} values as those corresponding to the CH_2 groups in the $C_{12}E_8$ tail. On the basis of the modeling results presented here, we conclude that care must be taken in applying the CS−MT model to surfactants with relatively long, polymeric heads. Without an accurate estimate of the appropriate g_{tr_i} values to use for the hydrophobic groups in the surfactant head, application of eq 2 to quantify the hydrophobic effect may not yield accurate results.

Although we do not explore these here, a number of approaches could be used to obtain more accurate estimates of g_{tr_i} values for the $C_{12}E_8$ head. Perhaps, the most straightforward approach would involve using an experimental or computational method to estimate the transfer free energy of an ethylene oxide monomer from bulk aqueous solution to a bulk phase of water and poly(ethylene oxide) molecules that serves as a reasonable proxy for the anisotropic corona region of the micelle. After obtaining the g_{tr_i} value of an ethylene oxide monomer, eq 2 could be used to calculate g_{dehydr}, albeit with the summation given in eq 2 extended to include all the hydrophobic groups in the $C_{12}E_8$ tail as well as all the ethylene oxide groups in the $C_{12}E_8$ head. To estimate g_{tr_i} of an ethylene oxide monomer, the solvation free energy of an ethylene oxide group in water and the solvation free energy of an ethylene oxide group in a bulk phase of water and poly(ethylene oxide) molecules could be determined experimentally. Alternatively, a theoretical approach could be used to estimate the transfer free energy or solvation free energy, for example, by using the Flory−Huggins approach with appropriate χ parameters or using a computer simulation approach that uses a realistic force field to describe interactions between the system components.[2,41]

4.9. Modeling Results for Decanoyl-*n*-Methylglucamide (MEGA-10). CS−MT modeling results for the simulated MEGA-10 micelle are reported in Table 3, and theoretical predictions made using the CS−MT model and the traditional MT model for the micellization behavior of MEGA-10 are reported in Table 4. Experimental data is also reported in Table 4 for comparison.[42] All data was generated for MEGA-10 in aqueous solution at 30 °C with 0.1 M of added NaCl. Each value reported in Tables 3 and 4 for MEGA-10 was computed using the approach described in Section 4.2. In applying the CS−MT model and the traditional MT model, the surfactant head area, a_h, was modeled as being equal to 62 Å^2.[8]

Computer simulation of MEGA-10 was conducted for a micelle with an aggregation number of 42. However, the optimal MEGA-10 micelle shape and size predicted by the CS−MT model are small spheres with a number-average aggregation number of only 22. As a result, the predicted value of g_{int} ($4.96k_BT$) is significantly higher than the predicted value of $\hat{g}_{int}$ ($3.81k_BT$). The low predicted aggregation number of MEGA-10 is due in part to its large head area, which at 62 Å^2 is larger than that of any of the other nonionic surfactants modeled here. This large head area, in turn, results in MEGA-10 having the highest value of g_{st} ($1.97k_BT$) among all the nonionic surfactants modeled. For MEGA-10, $g_{tr,CS-MT}$ ($-17.36k_BT$) is significantly more negative than g_{tr} ($-15.47k_BT$) computed using the traditional MT modeling approach. This is due primarily to the hydrophobic free-energy contributions calculated in the CS−MT modeling approach for groups 11 and 12 (see Figure 9). In the traditional MT modeling approach, the most reasonable estimate of the head and tail of MEGA-10 would be to include only groups 16−24 in the linear alkyl chain as part of the tail. On the basis of this tail assignment, the traditional MT model prediction of g_{tr} is less negative than the CS−MT model prediction of $g_{tr,CS-MT}$. As a result, the CMC predicted by the CS−MT model (6.55 mM) is much closer to the experimental CMC (5 mM) than the CMC predicted by the traditional MT model (43.33 mM). Clearly, only the CS−MT model predictions are reasonable for MEGA-10.

4.10. Effect of the Definition of Hydrating Contacts on the Modeling Results. In article 1, we stated that, in the context

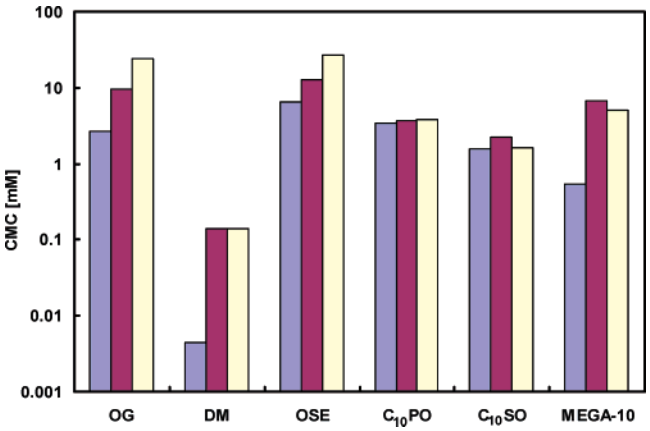

Figure 13. Comparison of CMCs predicted by the CS−MT model using f_{water} (blue) and f (maroon) values (see Section 4.10) in eqs 2 and 4 to compute g_{dehydr} and g_{hydr}, respectively. The definitions of f and f_{water} are given in Section 3.1. The experimental CMCs (yellow) are also reported for comparison with the theoretical predictions. The CMC values are reported on a log scale.

of CS−MT modeling, an atom in contact with a hydrophobic group is considered "hydrating" if the atom is capable of (i) forming hydrogen bonds or (ii) coordinate (dative covalent) bonding. On the basis of this definition, both water and hydrogen-bonding groups in surfactant heads contribute hydrating contacts when computing f, and therefore, one should use f values, rather than f_{water} values, in implementing the CS−MT modeling approach.

The effect of the way in which hydrating contacts are defined on our modeling results can be evaluated by comparing the CS−MT model predictions for the CMC using f values in eqs 2 and 4 with the CS−MT model predictions of the CMC using f_{water} values in eqs 2 and 4. Figure 13 compares the CMC predictions for OG, DM, OSE, $C_{10}PO$, $C_{10}SO$, and MEGA-10 using both approaches with the experimental CMC values. Results for $C_{12}E_8$ are not shown because the CS−MT model does not yield sufficiently accurate CMC predictions for this surfactant (for reasons discussed in Section 4.8). CMC results are reported on a log scale because of the large range spanned by the predicted and the experimental CMC values. With the exception of $C_{10}SO$, using f values (see the maroon results) in eqs 2 and 4 yields better CMC predictions than using f_{water} values (blue) in eqs 2 and 4. If only water molecules are considered to be hydrating, the degree of dehydration of the micelle core is overestimated, resulting in a prediction of g_{form} that is often significantly more negative than that predicted using the traditional MT model. As expected intuitively, the discrepancy between the f and f_{water} modeling results is largest for surfactants with many hydrogen-bonding groups in the surfactant head. For example, for OG, by defining hydration using f_{water} instead of using f, the predicted CMC is reduced by a factor of 3.6. For DM, defining hydration using f_{water} instead of using f has an even greater effect and reduces the predicted CMC by a factor of 31.

Modeling contacts with hydrogen-bonding groups in the surfactant head as being hydrating is consistent with the approximation made in traditional MT modeling that the surfactant heads at the micelle core−water interface shield only 21 Å^2 of the interface from hydrating contacts, an area corresponding to the cross-sectional area of the linear alkyl chain connected to the surfactant head, rather than to the cross-sectional area of the surfactant head. In traditional MT modeling, if the surfactant head is modeled as shielding its cross-sectional area, implying that the head itself does not provide hydrating contacts, less accurate predictions of micellization behavior would be obtained.

5. Conclusions

In this article, we have demonstrated the validity and accuracy of the CS−MT model by using it to model seven nonionic surfactants. To implement the CS−MT model, we have conducted two independent MD simulations for each nonionic surfactant to determine information about the changes in hydration that occur upon micelle formation. Changes in hydration were quantified by computing a fractional hydration value, f, for each group. The f values obtained for each surfactant through MD simulation were used as an input in a new model presented in article 1 of this series that computes the magnitude of the hydrophobic free-energy contribution as the sum of g_{dehydr} and g_{hydr}. In this article, we have used a simple computational strategy to estimate g_{dehydr} and g_{hydr} for each nonionic surfactant modeled. To calculate g_{dehydr}, g_{tr_i} values were estimated using the same solubility correlations for linear alkyl tails that our group has used in the past in traditional MT modeling.[32] To calculate g_{hydr}, we have made the simple approximation that this contribution is equal to zero for any hydrophobic group with a value of f greater than 0.60. For hydrophobic groups with a value of f less than 0.60, g_{hydr} was calculated using eq 4 and an expression for Δg_{wc} derived for oil molecules in article 1 of this series. By combining elements of the CS−MT model and the traditional MT model, the hydrophobic driving force for micelle formation was quantified as a transfer free energy ($g_{tr,CS-MT}$). After determining this input, the free energy of micelle formation, g_{form}, and the CMC were calculated for each surfactant for micelles of the optimal shape and size.

Reasonable agreement between the CS−MT model predictions and the experimental data for g_{form} and the CMC were obtained for OG, DM, OSE, $C_{10}PO$, $C_{10}SO$, and MEGA-10. For $C_{12}E_8$, the CS−MT model predictions were not in good agreement with the experimental data because the simple approximations that were made in this article to estimate g_{dehydr} were not sufficiently accurate for this surfactant. For the 16 hydrophobic CH_2 groups in the E_8 head of $C_{12}E_8$, we believe that more accurate values of g_{tr_i} must be used to obtain accurate modeling results. Consequently, we recommend that the simple approximations that we have made to compute g_{dehydr} only be used for surfactants with relatively small, non-polymeric heads.

The predictions of the CS−MT and the traditional MT modeling approaches were found to be in reasonable agreement for OG, DM, OSE, $C_{10}PO$, and $C_{10}SO$. For four of these surfactants (DM, OSE, $C_{10}PO$, and $C_{10}SO$), the CMCs predicted by the CS−MT model were closer to the experimental CMC values than the CMCs predicted by the traditional MT model. In addition, CMCs predicted for binary mixtures of $C_{10}PO$ and $C_{10}SO$ using the CS−MT modeling approach were significantly closer to the experimental CMCs than those predicted using the traditional MT modeling approach. The CMC predicted by the CS−MT model for MEGA-10 (6.55 mM) was significantly closer to the experimental CMC value (5 mM) than the CMC predicted by the traditional MT model (43.3 mM).

Using the f values obtained through computer simulation, we evaluated the accuracy of two approximations made in traditional MT modeling to quantify the hydrophobic driving force for micelle formation in aqueous solution for the first time. These include (i) the accuracy of using surfactant head and tail assignments to compute g_{tr} and (ii) the extent to which surfactant heads shield the micelle core from hydrating contacts. Approximation (i) was found to be reasonable for nonionic

surfactants in the absence of detailed hydration data. Approximation (ii) was found to be accurate for some of the nonionic surfactants modeled in this article but not very accurate for others. However, the approximation made in the traditional MT model that a surfactant head shields 21 Å^2 at the micelle core−water interface from hydrating contacts was found to be in close agreement with the average computer simulation estimate for this shielded area (21.85 Å^2). An important advantage of the CS−MT modeling approach is that it eliminates the need to make approximations (i) and (ii) by enabling determination of the changes in hydration that occur during micelle formation, as well as providing a theoretical model to quantify the hydrophobic driving force for micelle formation in aqueous solution directly from this hydration data.

Using the relatively simple approach to estimate g_{dehydr} and g_{hydr} presented in this article, the CS−MT model was found to yield similar, or superior, predictions of the CMCs of nonionic surfactants with relatively small, non-polymeric heads when compared to the traditional MT model. The results obtained for the relatively complex surfactant MEGA-10 highlight the strengths of the CS−MT modeling approach: for surfactants where it is difficult to make accurate head and tail assignments for traditional MT modeling and for surfactants where a significant number of hydrophobic groups are located near the aggregate core−water interface and are partially hydrated, the CS−MT modeling approach is expected to yield better results than the traditional MT modeling approach. Clearly, the more accurate predictions of the CS−MT model come at the cost of greater computational expense. Nevertheless, given the relatively small fraction of surfactants with sufficient structural and chemical simplicity to be easily modeled using the traditional MT model, we conclude that the CS−MT modeling approach represents a very promising alternative.

Acknowledgment. This research was supported in part by funding provided by DuPont through the DuPont−MIT Alliance. B.C.S. would like to thank Kate Stafford for her assistance in setting up several of the nonionic surfactant simulations. B.C.S. and A.G. are also grateful to Dr. Isaac Reif for critically reading the manuscript and for stimulating discussions about the CS−MT model.

Supporting Information Available: Two figures are available that plot SASA normalized by the average value of SASA as a function of simulation time during the 5 ns data-gathering simulation run (see Section 2.3) for each of the seven nonionic surfactant micelles simulated in this article. This material is available free of charge via the Internet at http://pubs.acs.org.

References and Notes

(1) Stephenson, B. C.; Goldsipe, A.; Beers, K. J.; Blankschtein, D. *J. Phys. Chem. B* **2007**, *111*, 1025−1044.
(2) Nagarajan, R.; Ruckenstein, E. *Langmuir* **1991**, *7*, 2934−2969.
(3) Shiloach, A.; Blankschtein, D. *Langmuir* **1998**, *14*, 1618−1636, and references cited therein.
(4) Gunnarsson, G.; Jonsson, B.; Wennerstrom, H. *J. Phys. Chem.* **1980**, *84*, 3114−3121.
(5) Jonsson, B.; Wennerstrom, H. *J. Colloid Interface Sci.* **1981**, *80*, 482−496.
(6) Evans, D. F.; Mitchell, D. J.; Ninham, B. W. *J. Phys. Chem.* **1984**, *88*, 6344−6348.
(7) Hayter, J. B. *Langmuir* **1992**, *8*, 2873−2876.
(8) Puvvada, S.; Blankschtein, D. *J. Chem. Phys.* **1990**, *92*, 3710−3724, and references cited therein.
(9) van der Spoel, D.; Lindahl, E.; Hess, B.; van Buuren, A. R,; Apol, E.; Meulenhoff, P. J.; Tieleman, D. P.; Sijbers, A. L. T. M.; Feenstra, K. A.; van Drunen, R.; Berendsen, H. J. C. *Gromacs User Manual version 3.2*; www.gromacs.org:2004.
(10) Goldsipe, A.; Blankschtein, D. *Langmuir* **2005**, *22*, 9850−9865, and references cited therein.
(11) Jorgensen, W. L.; Maxwell, D. S.; Tirado-Rives, J. *J. Am. Chem. Soc.* **1996**, *118*, 11225−11236.
(12) Chirlian, L. E.; Francl, M. M. *J. Comput. Chem.* **1987**, *8*, 894−905.
(13) Stephenson, B. C.; Beers, K.; Blankschtein, D. *Langmuir* **2006**, *22*, 1500−1513, and references cited therein.
(14) Stephenson, B. C.; Rangel-Yagui, C. O.; Pessoa, A.; Tavares, L. C.; Beers, K.; Blankschtein, D. *Langmuir* **2006**, *22*, 1514−1525.
(15) Darden, T.; York, D.; Pedersen, L. *J. Chem. Phys.* **1993**, *98*, 10089−10092.
(16) Essmann, U.; Perera, L.; Berkowitz, M. L.; Darden, T.; Lee, H.; Pedersen, L. G. *J. Chem. Phys.* **1995**, *103*, 8577−8593.
(17) Ryckaert, J. P.; Ciccotti, G.; Berendsen, H. J. C. *J. Comput. Phys.* **1997**, *23*, 327−341.
(18) Berendsen, H. J. C.; van der Spoel, D.; van Drunen, R. *Comput. Phys. Commun.* **1995**, *91*, 43−56.
(19) Lindahl, E.; Hess, B.; van der Spoel, D. *J. Mol. Model.* **2001**, *7*, 306−317.
(20) Jang, S. S.; Goddard, W. A., III *J. Phys. Chem. B* **2006**, *110*, 7992−8001.
(21) Stephenson, B. C.; Beers, K. J. *J. Phys. Chem. B* **2006**, *110*, 19393−19405.
(22) Feller, S.; Pastor, R. *Biophys. J.* **1996**, *71*, 1350−1355.
(23) Israelachvili, J. N. *Intermolecular and Surface Forces*, 2nd ed.; Academic Press: New York, 1991.
(24) Bruce, C.; Berkowitz, M.; Perera, L.; Forbes, M. D. E. *J. Phys. Chem. B* **2002**, *106*, 3788−3793.
(25) Flyvbjerg, H.; Petersen, H. G. *J. Chem. Phys*. **1989**, *91*, 461−466.
(26) Hess, B. Thesis. *Stochastic Concepts in Molecular Simulation*; Rijksuniversiteit Groningen, 1999.
(27) Hess, B. *J. Chem. Phys.* **2002**, *116*, 209−217.
(28) Gibbs, J. W. *The Scientific Papers of J. W. Gibbs*; Dover: New York, 1961; Vol. 1.
(29) Koenig, F. O. *J. Chem. Phys.* **1950**, *18*, 449.
(30) Buff, F. P. *J. Chem. Phys.* **1951**, *19*, 1591.
(31) Tolman, R. C. *J. Chem. Phys.* **1948**, *16*, 758.
(32) Smith, R.; Tanford, C. *Proc. Natl. Acad. Sci.* **1973**, *70*, 289−293.
(33) Reynolds, J. A.; Gilbert, D. B.; Tanford, C. *Proc. Natl. Acad. Sci.* **1974**, *71*, 2925−2927.
(34) Stephenson, B. C.; Beers, K. J.; Blankschtein, D. *J. Phys. Chem. B* **2007**, *111*, 1063−1075.
(35) Mukerjee, P.; Chan, C. C. *Langmuir* **2002**, *18*, 5375−5381.
(36) Srinivasan, V.; Blankschtein, D. *Langmuir* **2003**, *19*, 9932−9945, and references cited therein.
(37) Rosen, M. J.; Sulthana, S. B. *J. Colloid Interface Sci.* **2001**, *239*, 528−534.
(38) Aratono, M.; Kanda, T.; Motomura, K. *Langmuir* **1990**, *6*, 843−846.
(39) Holland, P. M.; Rubingh, D. N. *J. Phys. Chem.* **1983**, *87*, 1984−1990.
(40) Alargova, R. G.; Kochijashky, I. I.; Sierra, M. L.; Zana, R. *Langmuir* **1998**, *14*, 5412−5418.
(41) Carale, T. R.; Pham, Q. T.; Blankschtein, D. *Langmuir* **1994**, *10*, 109−121.
(42) Hierrezuelo, J. M.; Aguiar, J.; Ruiz, C. C. *Langmuir* **2004**, *20*, 10419−10426.